

PERFORMANCE ANALYSIS OF A COMPACT HEAT EXCHANGER

A THESIS SUBMITTED IN PARTIAL FULFILLMENT OF THE
REQUIREMENTS FOR THE DEGREE OF

**Master of Technology
in
Mechanical Engineering**

By

Akash Pandey



**Department of Mechanical Engineering
National Institute of Technology
Rourkela
2011**

PERFORMANCE ANALYSIS OF A COMPACT HEAT EXCHANGER

A THESIS SUBMITTED IN PARTIAL FULFILLMENT OF THE
REQUIREMENTS FOR THE DEGREE OF

**Master of Technology
in
Mechanical Engineering**

By

Akash Pandey

Under the Guidance of
Prof. Ranjit Kumar Sahoo



**Department of Mechanical Engineering
National Institute of Technology
Rourkela
2011**



National Institute of Technology

Rourkela

CERTIFICATE

This is to certify that the thesis entitled “**PERFORMANCE ANALYSIS OF A COMPACT HEAT EXCHANGER**” submitted to the National Institute of Technology, Rourkela (Deemed University) by **Akash Pandey**, Roll No. **209ME3227** for the award of the Degree of **Master of Technology** in **Mechanical Engineering** with specialization in “**Thermal Engineering**” is a record of bonafide research work carried out by him under my supervision and guidance. The results presented in this thesis has not been, to the best of my knowledge, submitted to any other University or Institute for the award of any degree or diploma.

The thesis, in my opinion, has reached the standards fulfilling the requirement for the award of the degree of **Master of technology** in accordance with regulations of the Institute.

Place: Rourkela

Date:

Dr. R. K. Sahoo

Professor

Department of Mechanical Engineering
National Institute of Technology, Rourkela

ACKNOWLEDGEMENT

I am extremely fortunate to be involved in an exciting and challenging research project like “**Performance Analysis of a Compact Heat Exchanger**”. It has enriched my life, giving me an opportunity to work in a new environment of Cryogenic heat transfer. This project increased my thinking and understanding capability and after the completion of this project, I experience the feeling of achievement and satisfaction.

I would like to express my greatest gratitude and respect to my supervisor **Prof. Ranjit Kumar Sahoo**, for his excellent guidance, valuable suggestions and endless support. He has not only been a wonderful supervisor but also a genuine person. I consider myself extremely lucky to be able to work under guidance of such a dynamic personality. Actually he is one of such genuine person for whom my words will not be enough to express.

I also express my special thanks to our research scholar **Mr. S. A. Alur, Mr. Balaji Kumar Choudhury**, and my best friend and classmate **Jitendra Bhushan** for their support during my experimentation. It was impossible for me to complete my project without their help. I would like to express my thanks to all my classmates, all staffs and faculty members of mechanical engineering department for making my stay in N.I.T. Rourkela a pleasant and memorable experience and also giving me absolute working environment where I unleashed ,my potential .

Last but not the least; I want to convey my heartiest gratitude to my parents for their immeasurable love, support and encouragement.

Date:

Akash Pandey
Roll. No. 209ME3227
M.tech. (Thermal Engg.)

CONTENTS

CERTIFICATE	i
ACKNOWLEDGEMENT	ii
CONTENTS	iii
ABSTRACT	vi
LIST OF FIGURES	vii
LIST OF TABLES	ix
NOMENCLATURE	x
CHAPTER 1	1
1. INTRODUCTION	2
1.1 Plate Fin Heat Exchanger	3
1.1.1 Advantages and Disadvantages	4
1.1.2 Materials	5
1.1.3 Manufacture	5
1.1.4 Applications	6
1.1.5 Flow arrangement	7
1.2 Plate Fin Heat transfer surfaces	10
1.2.1 Plain fins	11
1.2.2 Wavy fins	12
1.2.3 Offset Strip fins	12
1.2.4 Louvered fins	13
1.2.5 Perforated fins	14
1.2.6 Pin fins	14
1.3 Heat Transfer and Flow Friction Characteristics	15
1.4 Objectives of the Study	16

1.5 Organization of the Thesis	17
CHAPTER 2	18
2. LITERATURE SURVEY	18
CHAPTER 3	27
3. EXPERIMENTAL SETUP AND PROCEDURE	27
3.1 Detailed description of various equipment's and instruments used	27
3.1.1 Plate Fin Heat Exchanger	27
3.1.2 Twin Screw Compressor	30
3.1.3 Heating Element	31
3.1.4 Resistance Temperature Detector (RTDs)	31
3.1.5 Orifice Mass Flow Meter	35
3.1.6 Variac or Autotransformer	36
3.2 Test Rig	37
3.2.1 Procedure for Hot Testing	39
CHAPTER 4	40
4. RATING PROCEDURE	40
CHAPTER 5	47
5. PERFORMANCE ANALYSIS	47
5.1 Calculations	48
5.2 Variation of Effectiveness with Mass Flow Rate	50
5.3 Variation Overall Thermal Conductance with Mas Flow Rate	51
5.4 Variation of Hot and Cold Effectiveness with Mass Flow Rate	52
5.5 Variation of Pressure Drop with Mass Flow Rate	53
CHAPTER 6	54
6. CONCLUSION	54

6.1 Scope for Future Work	54
7. REFERENCES	55

ABSTRACT

Compact heat exchangers are one of the most critical components of many cryogenic components; they are characterized by a high heat transfer surface area per unit volume of the exchanger. The heat exchangers having surface area density (β) greater than 700 m²/m³ in either one or more sides of two-stream or multi stream heat exchanger is called as a compact heat exchanger. Plate fin heat exchanger is a type of compact heat exchanger which is widely used in automobiles, cryogenics, space applications and chemical industries. The plate fin heat exchangers are mostly used for the nitrogen liquefiers, so they need to be highly efficient because no liquid nitrogen is produced, if the effectiveness of heat exchanger is less than 87%. So it becomes necessary to test the effectiveness of these heat exchangers before putting them in to operation.

The available plate fin heat exchanger has rectangular offset strip geometry and is tested in the laboratory using the heat exchanger test rig. The experiment is conducted under balanced condition i.e. the mass flow rate for both sides of fluid stream is same, and the experiment is carried out at different mass flow rates. The effectiveness of heat exchanger is found out for different mass flow rates. Various correlations are available in the literature for estimation of heat transfer and flow friction characteristics of the plate fin heat exchanger, so the various performance parameters like effectiveness, heat transfer coefficient and pressure drop obtained through experiments is compared with the values obtained from the different correlations. The longitudinal heat conduction through walls decreases the heat exchanger effectiveness, especially of cryogenic heat exchangers, so the effectiveness and overall heat transfer coefficient is found out by considering the effect of longitudinal heat conduction using the Kroeger's equation.

LIST OF FIGURES

Figure No.	Title	Page no.
CHAPTER 1		
1.1	Basic Heat Transfer Mechanism	2
1.2	Exploded View of a Plate Fin Heat Exchanger	4
1.3	Cross Flow arrangement	8
1.4	Counter Flow arrangement	8
1.5	Cross Counter Flow arrangement	9
1.6	Some of the common Fin Geometries	10
1.7	Details of Boundary layer and Flow across Offset Strip and Wavy Fin	11
CHAPTER 2		
2.1	Typical j and f characteristics	19
2.2	Laminar Flow on the Fins and in the Wakes	20
2.3	Laminar Flow on the Fins and Oscillating Flow on the Wakes	20
CHAPTER 3		
3.1	Manufacturing details of plate Fin Heat Exchanger	29
3.2	Working Mechanism of Plate Fin Heat Exchanger	30
3.3	RTDs Construction	32
3.4	RTD Calibration Graph	33
3.5	Orifice Plate	35
3.6	Schematic P&I diagram of the Experimental Test Rig	37
3.7	Photograph of Experimental test rig	38
CHAPTER 4		
4.1	Geometry of Typical Offset Strip Fin Surface	41
CHAPTER 5		
5.1	Variation of Effectiveness with Mass flow rate (hot inlet temp. = 96°C)	50

5.2	Variation of Effectiveness with Mass flow rat (hot inlet temp. = 66°C)	50
5.3	Variation of Overall Thermal conductance with Mass flow rate (hot inlet Temperature = 96°C)	51
5.4	Variation of Overall Thermal conductance with Mass flow rate (hot inlet Temperature = 66°C)	51
5.5	Variation of Hot and Cold Effectiveness with Mass flow rate (hot inlet Temperature = 96°C)	52
5.6	Variation of Hot and Cold Effectiveness with Mass flow rate (hot inlet Temperature = 66°C)	52
5.7	Variation of Pressure Drop with Mass Flow Rate	53

LIST OF TABLES

Table No.	Title	Page No.
CHAPTER 2		
2.1	Chronological listings of the correlations of OSF channels	24
CHAPTER 3		
3.1(a)	Dimension of Procured Plate Fin Heat Exchanger	27
3.1(b)	Dimension of Procured Plate Fin Heat Exchanger	28
3.2	Procured Design data of Plate Fin Heat Exchanger	28
3.3	Calibration Chart	34
CHAPTER 4		
4.1	Core Data	41
CHAPTER 5		
5.1	Experimentally Observed Data	47
5.2	Performance of Heat Exchanger	49

NOMENCLATURE

NTU = no. of transfer units

Re = Reynolds number

T = Temperature

C = Specific heat

P = Pressure

U = Overall heat transfer coefficient

h = Heat transfer Coefficient

j = Colburn factor

f = Friction factor

ε = Effectiveness

η = Efficiency

h = hot fluid

c = cold fluid

A_o = Total heat transfer surface area

1 = inlet

2 = outlet

R = Gas constant

D_e = Equivalent Diameter

CHAPTER 1

Introduction

INTRODUCTION

A heat exchanger is a device to transfer heat from a hot fluid to cold fluid across an impermeable wall. Fundamental of heat exchanger principle is to facilitate an efficient heat flow from hot fluid to cold fluid. This heat flow is a direct function of the temperature difference between the two fluids, the area where heat is transferred, and the conductive/convective properties of the fluid and the flow state. This relation was formulated by Newton and called Newton's law of cooling, which is given in Equation (1.1)

$$Q = h \cdot A \cdot \Delta T \quad \dots\dots\dots (1.1)$$

Where h is the heat transfer coefficient [W/m²K], where fluid's conductive/convective properties and the flow state comes in the picture, A is the heat transfer area [m²], and T is the temperature difference [K].Figure. 1.1 shows the basic heat transfer mechanism

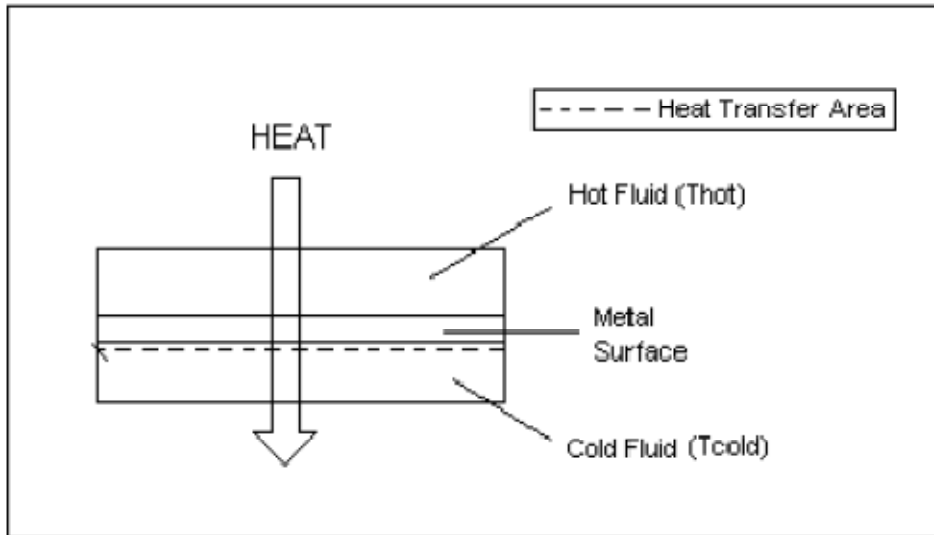


Fig. 1.1 Basic heat transfer mechanism

Heat exchangers are one of the vital components in diverse engineering plants and systems. So the design and construction of heat exchangers is often vital for the proper functioning of such systems. It has been shown in [Barron, 1985] that the low temperature plants based on Linde – Hampson cycle cease to produce liquid if the effectiveness of the heat

exchanger is below 86.9%. On the other hand in aircrafts and automobiles, for a given heat duty, the volume and weight of the heat exchangers should be as minimum as possible.

So the main requirement for any heat exchanger is that it should be able to transfer the required amount of heat with a very high effectiveness. In order to increase the heat transfer in a basic heat exchanger mechanism shown below in Figure 1.1, assuming that the heat transfer coefficient cannot be changed, the area or the temperature differences have to be increased. Usually, the best solution is that the heat transfer surface area is extended although increasing the temperature difference is logical, too. In reality, it may not be much meaningful to increase the temperature difference because either a hotter fluid should be supplied to the heat exchanger or the heat should be transferred to a colder fluid where neither of them are usually available. For both cases either to supply the hot fluid at high temperature or cold fluid at lower temperature extra work has to be done. Furthermore increasing the temperature difference more than enough will cause unwanted thermal stresses on the metal surfaces between two fluids. This usually results in the deformation and also decreases the life span of those materials. As a result of these facts, increasing the heat transfer surface area generally is the best engineering approach.

The above requirements have been the motivation for the development of a separate class of heat exchangers known as Compact heat exchangers. These heat exchangers have a very high heat transfer surface area with respect to their volume and are associated with high heat transfer coefficients. Typically, the heat exchanger is called compact if the surface area density (β) i.e. heat transfer surface area per unit volume is greater than $700 \text{ m}^2/\text{m}^3$ in either one or more sides of two-stream or multi stream heat exchanger [R.K Shah, Heat Exchangers, Thermal Hydraulic 1980]. The compact heat exchangers are lightweight and also have much smaller footprint, so they are highly desirable in many applications.

1.1 Plate fin heat exchanger

Plate fin exchanger is a type of compact heat exchanger where the heat transfer surface area is enhanced by providing the extended metal surface interface between the two fluids and is called as the fins. Out of the various compact heat exchangers, plate-fin heat exchangers are unique due to their construction and performance. They are characterized by high effectiveness, compactness, low weight and moderate cost. As the name suggests, a plate fin heat exchanger (PFHE) is a type of compact exchanger that consists of a stack of alternate flat plates called

parting sheets and corrugated fins brazed together as a block. Streams exchange heat by flowing along the passages made by the fins between the parting sheets. Separating plate acts as the primary heat transfer surface and the appendages known as fins act as the secondary heat transfer surfaces intimately connected to the primary surface. Fins not only form the extended heat transfer surfaces, but also work as strength supporting member against the internal pressure. The side bars prevent the fluid to spill over and mix with the second fluid. The fins and side bars are brazed with the parting sheet to ensure good thermal link and to provide the mechanical stability. Figure. 1.2 shows the exploded view of two layers of a plate fin heat exchanger. Such layers are arranged together in a monolithic block to form a heat exchanger.

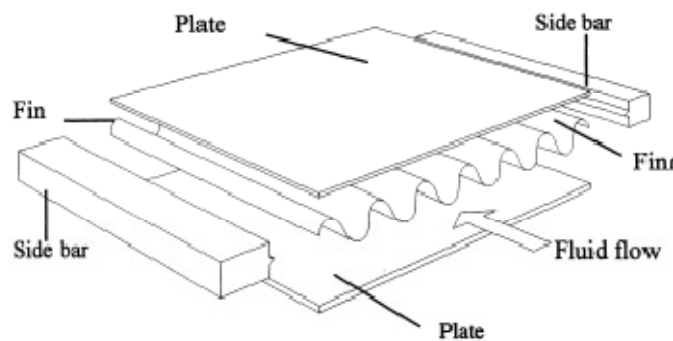


Fig. 1.2 Exploded view of a plate fin heat exchanger

1.1.1 Advantages and Disadvantages

Plate fin heat exchangers offer several advantages over the other heat exchangers:

1. **Compactness:** Large heat transfer surface area per unit volume (Typically $1000 \text{ m}^2/\text{m}^3$), is usually provided by the plate fin heat exchanger. This in turn produces a high overall heat transfer coefficient due to the heat transfer associated with the narrow passages and corrugated surfaces.
2. **Effectiveness:** very high thermal effectiveness more than 95% can be obtained.
3. **Temperature control:** The plate heat exchanger can operate with relatively small temperature differences. A close temperature approach (Temperature approach as low as 3K between single phase fluid streams and 1K between boiling and condensing fluids is

fairly common.), This is an advantage when high temperatures must be avoided. Local overheating and possibility of stagnant zones can also be reduced by the form of the flow passage.

4. **Flexibility:** Changes can be made to heat exchanger performance by utilizing a wide range of fluids and conditions that can be modified to adapt to the various design specifications. Multi stream operation is possible upto 10 streams.
5. True counter-flow operation (Unlike the shell and tube heat exchanger, where the shell side flow is usually a mixture of cross and counter flow.).

The main disadvantages of a plate fin heat exchanger are:

1. Limited range of temperature and pressure.
2. Difficulty in cleaning of passages, which limits its application to clean and relatively non-corrosive fluids, and
3. Difficulty of repair in case of failure or leakage between passages.

1.1.2 Materials

Plate fin heat exchangers are generally, made from an alloy of aluminum or stainless steel. However, the process temperature and pressure dictates the choice of the material. Aluminum alloys are particularly suitable for low temperature applications because of their low weight and excellent ductility and increasing strength under such conditions. In general, the fins or secondary surfaces and the side bars are usually joined to the separating plate by using dip brazing technology or more recently vacuum brazing technique. The brazing material in case of aluminum exchangers is an aluminum alloy of lower melting point, while that used in stainless steel exchangers is a nickel based alloy with appropriate melting and welding characteristics.

1.1.3 Manufacture

The basic principles of plate fin heat exchanger manufacture are the same for all sizes and all materials. The heat exchanger is assembled from a series of flat sheets and corrugated fins in a sandwich construction. Separating plates (i.e. parting sheets) provide the primary heat transfer surface. Separating plates are positioned alternatively with the layers of fins in the stack to form the containment between individual layers. These elements i.e. the corrugations, side-bars, parting sheets and cap sheets are now held together in a jig under a predefined load, and

placed in a furnace and brazed to form the plate fin heat exchanger block. After this the header tanks and nozzles are welded to the block, taking care that the brazed joints remain intact during the welding process. Differences arise in the manner in which the brazing process is carried out. The methods in common use are salt bath brazing and vacuum brazing. In the salt bath process, the stacked assembly is preheated in a furnace to about 550 C, and then dipped into a bath of fused salt composed mainly of fluorides or chlorides of alkali metals. The molten salt works as both flux and heating agent, maintaining the furnace at a uniform temperature. In case of heat exchangers made up of aluminum, the molten salt removes grease and the tenacious layer of aluminum oxide, which would otherwise weaken the joints. Brazing takes place in the bath when the temperature is raised above the melting point of the brazing alloy. The brazed block is cleansed of the residual solidified salt by dissolving in water, and is then thoroughly dried.

In the vacuum brazing process, no flux or separate pre-heating furnace is required. The assembled block is heated to brazing temperature by radiation from electric heaters and by conduction from the exposed surfaces into the interior of the block. The absence of oxygen in the brazing environment is ensured by application of high vacuum (Pressure $\approx 10^{-6}$ Mbar). The composition of the residual gas is further improved (lower oxygen content) by alternate evacuation and filling with an inert gas as many times as experience dictates. No washing or drying of the brazed block is required. Many metals, such as aluminum, stainless steel, copper and nickel alloys can be brazed satisfactorily in a vacuum furnace.

1.1.4 Applications

The plate-fin heat exchanger is suitable for use over a wide range of temperatures and pressures for gas-gas, gas-liquid and multi-phase duties. They are used in a variety of applications. They are mainly employed in the field of cryogenics for cryogenic separation and liquefaction of air, natural gas processing and liquefaction, production of petrochemicals and large refrigeration systems. The exchangers that are used for cryogenic air separation and LPG fractionation are the largest and most complex units of the plate fin type and a single unit could be of several meters in length. Brazed aluminum plate fin exchangers are widely used in the aerospace industries because of their low weight to volume ratio and compactness. They are being used mainly in environment control system of the aircraft, avionics and hydraulic oil cooling and fuel heating. Making heat exchangers as compact as possible has been an everlasting

demand in automobile and air conditioning industries as both are space conscious. In the automobile sector they are used for making the radiators. The other miscellaneous applications are:

1. Fuel cells
2. Process heat exchangers.
3. Heat recovery plants.
4. Pollution control systems
5. Fuel processing and conditioning plants.
6. Ethylene and propylene production plants.

1.1.5 Flow arrangement

A plate fin heat exchanger can have two or more than two streams, which may flow in directions parallel or perpendicular to one another. When the flow directions are parallel, the streams may flow in the same or in opposite sense. So there are three primary flow arrangements for a plate fin heat exchanger – (i) parallel flow, (ii) counter-flow and (iii) cross flow. Thermodynamically, the counter-flow arrangement provides the highest heat (or cold) recovery, while the parallel flow geometry gives the lowest. While the cross flow arrangement, gives an intermediate thermodynamic performance, by offering superior heat transfer properties and easier mechanical layout. Under some circumstances, a hybrid cross – counter-flow geometry provides greater heat (or cold) recovery with superior heat transfer performance. Thus in general engineering practice, there are three main configurations for the plate fin heat exchangers: (a) cross flow, (b) counter-flow and (c) cross-counter flow.

(a) Cross flow:

In this type of heat exchangers as shown in the Fig. (1.3) the fluids flow in directions normal to each other. Thermodynamically the effectiveness for cross flow heat exchangers falls in between that for the counter flow and parallel flow arrangements. The largest structural temperature difference exists at the corner of the entering hot and cold fluids. Only two streams are handled, in a cross flow type of a heat exchanger which eliminates the need for distributors. For this type of heat exchangers the header tanks are located on all four sides of the heat exchanger core, making this arrangement simple and cheap. If high effectiveness is not necessary, and if the two fluid streams have widely differing volume flow rates, or if either one or both streams are nearly isothermal (as in

single component condensing or boiling), then the cross flow arrangement should be preferred. Typical applications include automobile radiators and some aircraft heat exchangers. (Fig.1.3 shows a cross flow arrangement).

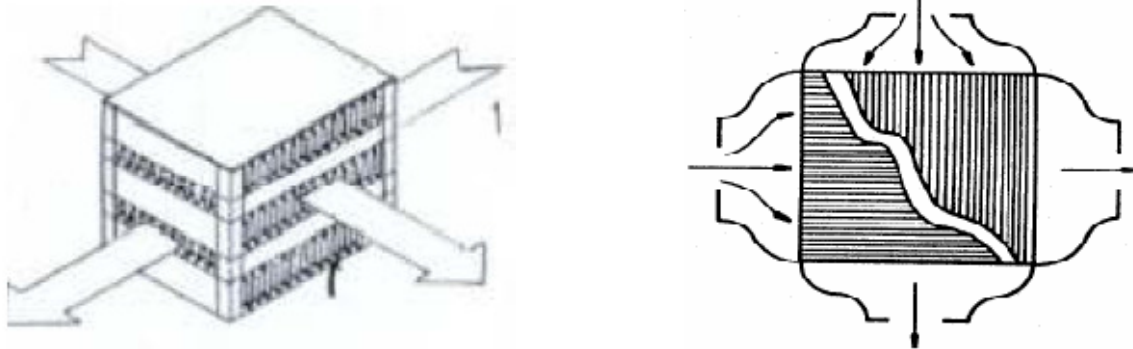


Fig.1.3 Cross flow arrangement

(b) Counter flow:

In a counter flow heat exchanger the two fluids flow parallel to each other but in opposite directions. The counter-flow heat exchanger provides the most thermally effective arrangement for recovery of heat or cold from process streams. A counter flow arrangement is thermodynamically superior to any other flow arrangement. It is the most efficient flow arrangement, producing the highest temperature change in each fluid compared to any other two-fluid arrangement for a given overall thermal conductance (UA), fluid flow rates and fluid inlet temperatures. Cryogenic refrigeration and liquefaction equipment use this geometry almost exclusively. But this type of heat exchangers demands proper design because of the complex geometry of headers. (Fig. 1.4 shows a counter flow arrangement for heat exchanger)

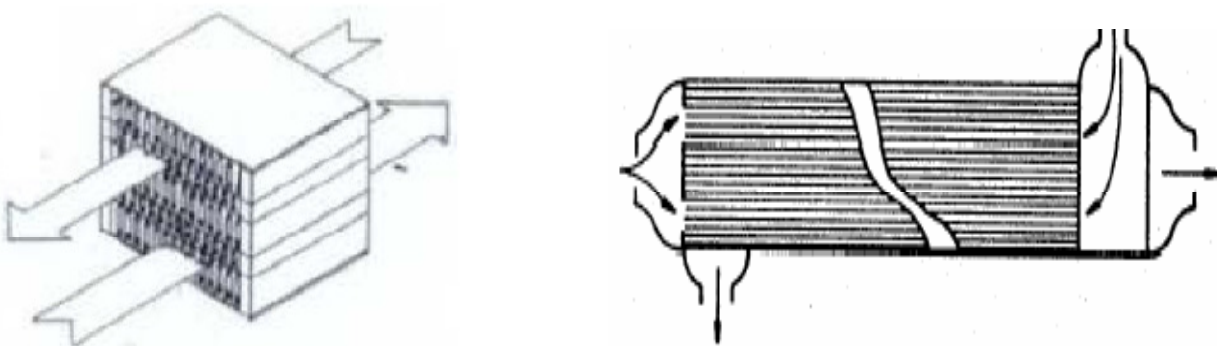


Fig.1.4 Counter flow arrangement

(c) Cross-Counter flow:

The cross-counter flow geometry is a hybrid of counter-flow and cross flow arrangements, delivering the thermal effectiveness of counter-flow heat exchanger with the superior heat transfer characteristics of the cross flow configuration. In this arrangement, one of the streams flows in a straight path, whereas the second stream follows a zigzag path normal to that of the first stream. While moving along the zigzag path, the second fluid stream covers the length of the heat exchanger in a direction opposite to that of the direct stream. Thus the flow pattern can be assumed to be globally counter-flow while remaining locally cross flow. Cross-counter flow PFHEs are used in applications similar to those of simple cross flow exchangers, but they allow more flexibility in design and fabrication. They are particularly suited for the applications where the two streams have considerably different volume flow rates, or permit significantly different pressure drops. The fluid with the larger volume flow rate or that with the smaller value of allowable pressure drop is made to flow through the straight channel, while the other stream follows the zigzag path. For example, in a liquid-to-gas heat exchanger, the gas stream with a large volume flow rate and low allowable pressure drop is assigned the straight path, while the liquid stream with a high allowable pressure drop flows normal to it over a zigzag path. This arrangement optimizes the overall geometry. (Fig.1.5 shows a cross-counter flow arrangement for heat exchanger)

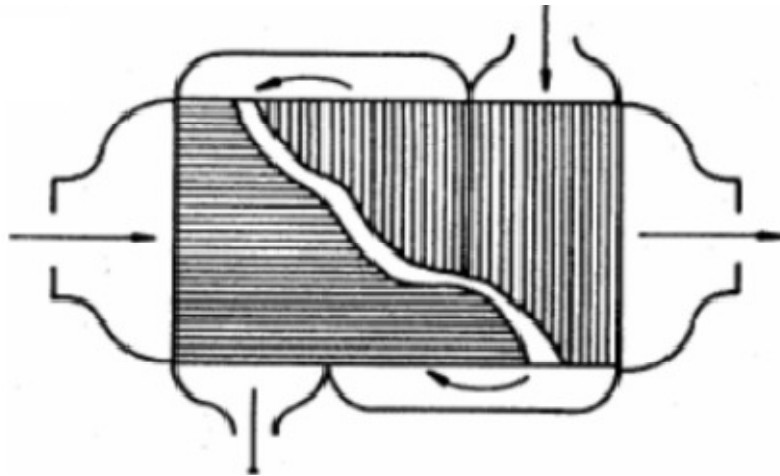


Fig.1.5 Cross-counter flow arrangement

1.2 Plate Fin heat transfer surfaces

The plate fin exchangers are mainly employed for liquid-to-gas and gas-to-gas applications. Due to the low heat transfer coefficients in gas flows, extended surfaces are commonly employed in plate-fin heat exchangers. By using specially configured extended surfaces, heat transfer coefficients can also be enhanced. While such special surface geometries provide much higher heat transfer coefficients than plain extended surfaces, but at the same time, the pressure drop penalties are also high, though they may not be severe enough to negate the thermal benefits. A variety of extended surfaces like the plain trapezoidal, plain rectangular shown in Fig. 1.6 can perform such function, and we have included the offset strip fin geometry in our present work.

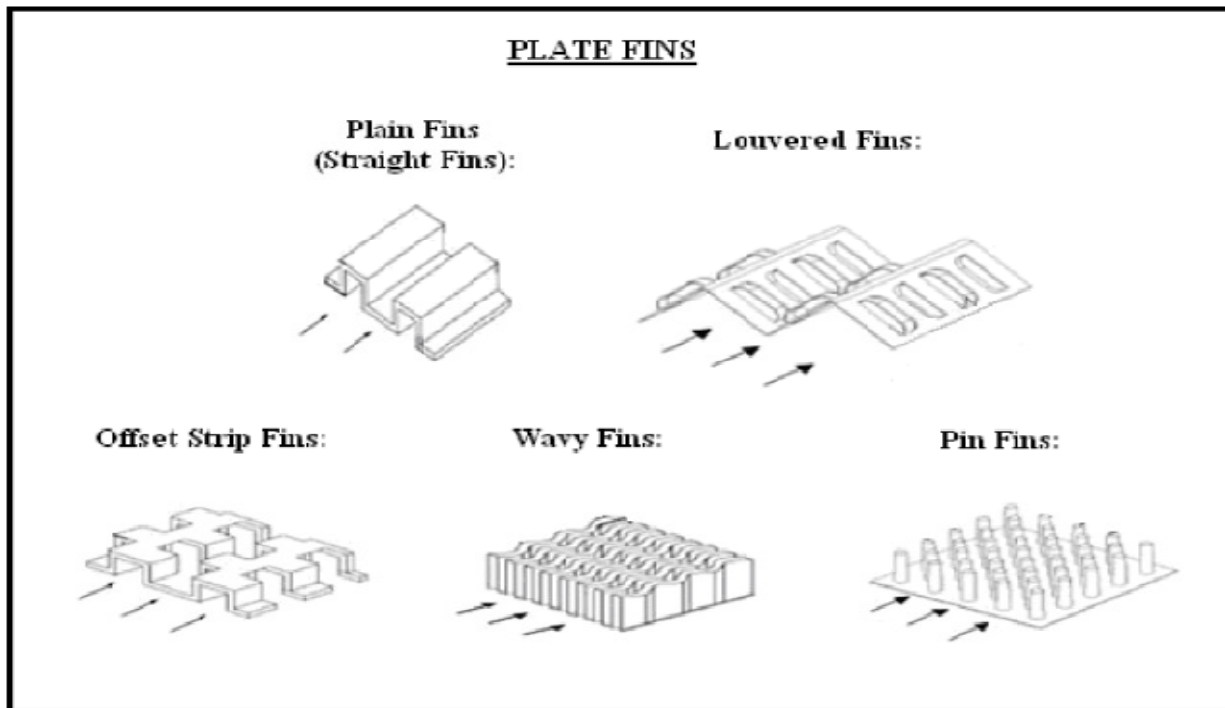


Fig.1.6 some of the common fin geometries

In order to improve the gas side coefficients, surface features are needed to be provided on the gas side coefficients. These features may be divided into two categories: the first, in which the surface remains continuous (wavy and herring-bone fins) and the second in which it is cut (offset, louvered). In a continuous type fin, the corrugations cause the gas to make sudden direction changes so that locally, the velocity and temperature gradients

are increased (Figure 1.7). This results in local enhancement of heat transfer coefficient. But an undesirable consequence of such enhancement in heat transfer coefficient is an increase in the friction factor and pressure drop

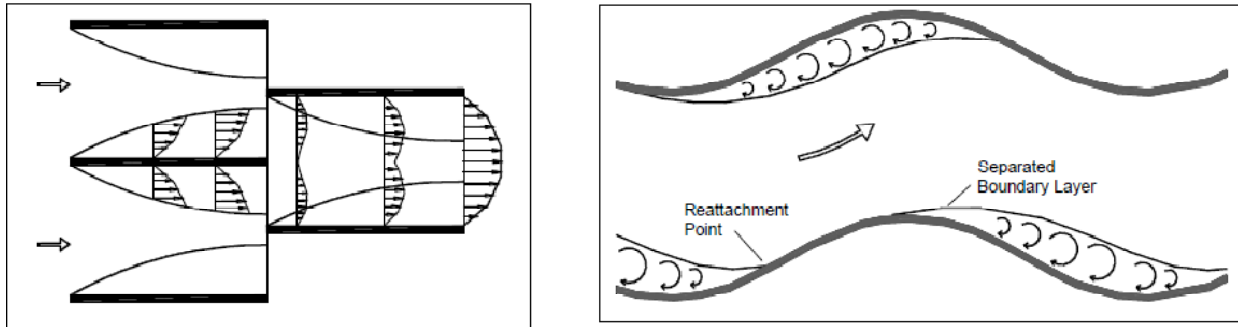


Fig 1.7 Details of boundary layer and flow across offset strip and wavy fin.

Whereas in a discontinuous type of fin geometry, boundary layers are interrupted which would form on a continuous plate. Adjacent to the leading edge of the fin, both heat transfer coefficients and friction factors are very much high due to generation of fresh boundary layers. But in addition to this friction drag, form drag is also formed due to the finite thickness of the fin. Although, the friction drag is associated with high heat transfer coefficient form drag has no counterpart and represents the form of wasted energy. The form drag could be substantial depending on the quality of the cutting edge. However, machined-formed fins are generally free from this problem. Brief descriptions of application and associated mechanism of the extended surfaces or fins depicted in Figure. 1.6 are given below.

1.2.1 Plain Fins

Plain fins are by far the most common of all compact cores or surfaces used in compact heat exchangers. The plain- fin surfaces are characterized by long uninterrupted flow passages, with performance similar to that obtained inside long circular tubes (Kays and London, 1984). Although passages of triangular and rectangular cross section are more common, any desired shape can be given to the fins, considering only manufacturing constraints. Straight fins in triangular arrangement can be manufactured at high speeds and hence are less expensive than rectangular fins. But generally they are structurally weaker than rectangular fins for the same passage size and fin thickness. They also have lower heat transfer performance compared to rectangular fins, particularly in laminar flow.

Plain fins are used in those applications where core pressure drop is critical. Their application range from aerospace air conditioning duties to oil refining (Hesselgreaves 2001), among many others. An heat exchanger with plain fins requires a smaller flow frontal area than that with interrupted fins for specified pressure drop, heat transfer and mass flow rate. Of course, the required passage length is higher leading to a larger overall volume. The heat transfer enhancement achieved with plain fins results mainly from increased area density, rather than any substantial rise in the heat transfer coefficient (Brockmeier, et al. 1993).

1.2.2 Wavy Fins

Wavy fins are uninterrupted fin surfaces with cross-sectional shapes similar to those of plain fins, but with cyclic lateral shifts perpendicular to the flow direction. The resulting wave form provides effective interruptions which causes the flow direction to change periodically and induces a complex flow field. Consequently, the boundary layer separates and reattaches periodically around the trough regions to promote enhanced heat transfer; increased pressure drop penalty is also accompanied. Actually the Heat transfer is enhanced due to creation of Goertler vortices. These counter-rotating vortices form while the fluid passes over the concave wave surfaces, and produce a corkscrew-like flow pattern.

The heat transfer and pressure drop characteristics of a wavy fin surface lie between those of plain and offset strip fins. The friction factor continues to fall with increasing Reynolds number. Wavy fins are common in the hydrocarbon industry where exchangers are designed with high mass velocities and moderate thermal duties. Unlike offset strip fins, the thickness of wavy fins is not limited at high fin densities. Therefore, wavy fins are often used for streams at high pressure, particularly those which can tolerate somewhat poor heat transfer coefficient.

1.2.3 Offset Strip fins

This is the most widely used fin geometry in high performance plate fin heat exchangers. It consists of a type of interrupted surface, which may be visualized as a set of plain fins cut normal to the flow direction at regular intervals, each segment being offset laterally by half the fin spacing. Typical strip lengths are 3-6mm, and the Reynolds number based on strip length is very small, which makes the flow to be always in laminar regime. The laminar boundary layer develops on the short strip length, and then dissipates in the wake region between successive

offset strips. Surface interruption enhances heat transfer by two independent mechanisms. First, it prevents the continuous growth of thermal boundary layer by periodically interrupting it. The thinner boundary layer offers lower thermal resistance compared to continuous fin types. Above a critical Reynolds number, interrupted surfaces offer an additional mechanism of heat transfer enhancement. Oscillations in the flow field in the form of vortices shed from the trailing edges of the interrupted fins enhance local heat transfer by continuously bringing in fresh fluid towards the heat transfer surfaces but this enhancement is accompanied by an increase in pressure drop. Considerable heat transfer enhancement is achieved compared to that of the plain fin. The heat transfer performance of an offset strip fin is often as much as 5 times that of a plain fin surface of comparable geometry, but at the expense of higher pressure drop. For specified heat transfer and pressure drop requirements, the offset strip fin surface demands a somewhat higher frontal area compared to those with plain fin, but results in a shorter flow length and lower overall volume. It is believed that with the shorter strip lengths, the better heat transfer performance is achieved (Manglik and Bergles, 1995).

An undesirable characteristic of this type of fin is that at high Reynolds numbers the friction factor remains nearly constant (because of the higher contribution of form drag), while the heat transfer performance goes down. Therefore, offset strip fins are used less frequently in very high Reynolds number applications. On the other hand, they are extensively used in air separation and other cryogenic applications where mass velocities are low and high thermal effectiveness is essential.

1.2.4 Louvered Fin

The louvered fin geometry bears a similarity to the offset strip fin. Instead of shifting the slit strips laterally, small segments of the fin are slit and rotated 20 to 45 degrees relative to the flow direction. Actually the fin surfaces are cut and bent out into the flow stream at frequent intervals in a louver or lanced-like fashion. The purpose of this fin surface louvers like a “venetian blind” is to break up the boundary layers so as to yield high heat transfer coefficients when compared to those in plain fins under same flow conditions (Kays and London, 1984). It has been contended that the performance of the louvered fins is similar to or better than offset-strip fins. The flow structure in the louvered fin flow passage is dependent on the flow rate Re at very low flow rate, the main flow stream does not pass through the louvers, whereas at high flow

rate the flow becomes nearly parallel to the louvers (Webb, 1994, and Davenport 1983). The base surface of the louvered fin geometry can be of triangular or rectangular shape, and louvers can be cut in many different forms.

The multi-louvered fin has the highest heat transfer enhancement relative to pressure drop in comparison with most other fin types. Flow over louvered fin surfaces is similar in nature to that through the offset strip fin geometry, with boundary layer interruption and vortex shedding playing major roles. An important aspect of louvered fin performance is the degree to which the flow follows the louver. Louvered fins are widely used in automotive heaters and radiators, where the latter is configured as a tube- fin exchanger.

1.2.5 Perforated Fins

This surface geometry is made by punching a pattern of spaced holes in the fin material before it is formed into flow channels. The channels may be triangular or rectangular in shape with either round or rectangular perforations. If the porosity of the resulting surface is sufficiently high, enhancement can occur due to boundary layer dissipation in the wake region formed by the holes (Webb, 1994). The performance of the perforated fin is less than that of a good offset strip fin, and thus the perforated fin is rarely used today. Perforated fins are now used only in limited number of applications such as turbulators in oil coolers. Furthermore, the perforated fin represents a wasteful way of making an enhanced surface, since the material removed in making the perforated hole is wasted.

1.2.6 Pin Fin

In a pin fin exchanger, a large number of small pins are sandwiched between plates in either an inline or staggered arrangement. Pins may have a round, an elliptical, or a rectangular cross section. Due to their low compactness and high cost per unit surface area compared to multi-louvered or offset strip fins these types of finned surfaces are not widely used these days. Due to vortex shedding behind the pins, noise and flow-induced vibration are produced, which are generally not acceptable in most heat exchanger applications. The potential application of pin fin surfaces is at low flow velocities ($Re < 500$), where pressure drop is negligible. Pin fins are used as electronic cooling devices with free-convection flow on the pin fin side.

1.3 Heat transfer and Flow Friction Characteristics

Accurate and reliable dimensionless heat transfer and pressure drop characteristics are a key input for designing or analyzing a plate fin heat exchanger. For single-phase flow, the heat transfer coefficient is generally expressed in terms of the Colburn correlation [Kern and Kraus, 1972]

$$h = j C_p G (\text{Pr})^{-2/3} \quad (1.2)$$

Where j called as colburn factor separates the effects of the fluid properties on the heat transfer coefficient and permits correlations as a function of the Reynolds number (Re). While the j data are expressed as functions of Prandtl number (Pr) and Re, temperature does not appear directly in the expression. Temperature has the only role in determining the thermo-physical properties such as density, viscosity, specific heat and thermal conductivity. Therefore, it is generally recognized that j data determined at one temperature / pressure level and expressed in dimensionless form are directly usable at another temperature / pressure level.

Since the plate fin heat exchangers are mainly used for gas to gas heat transfer applications and most of the gases are low density gases, so the pumping power requirement in a gas-to-gas heat exchanger is high as compared to that in a liquid-to-liquid heat exchanger. This fact makes it mandatory to have an accurate estimation of friction characteristics of the heat exchanger surfaces in gas application. The friction factor is defined on the basis of an equivalent shear force in the flow direction per unit friction area. This shear force can be either viscous shear (skin friction) or pressure force (form drag) or a combination of both. So without making an attempt to differentiate between them, it is possible to express them by Fanning friction factor (f) given by

$$f = \frac{\tau_s}{1/2\rho V^2} \quad (1.3)$$

While equation (1.3) is the basic definition of friction factor, the pressure drop (ΔP) for internal flow through the ducts can be calculated from equation (1.4)

$$\Delta P = \frac{2fLG^2}{2D_h} \quad (1.4)$$

It can be seen that temperature does not appear directly in the expression of friction factor also. Therefore, the f data determined at one temperature / pressure level are directly usable at

other temperature / pressure level. But it is seen that j and f are strong functions of fin geometries like fin height, fin spacing, fin thickness etc. Because fins are available in varied shapes, it becomes necessary to test each configuration individually to determine the heat transfer and flow friction characteristics for specific surface. For a given fin geometry, in general, increase in heat transfer performance is associated with increase in flow friction and vice versa. Customarily the ratio of j/f is taken as a measure of the goodness of the fin surface. Though the preferred fin geometry would have high heat transfer coefficient without correspondingly increased pressure penalty, the selection of particular fin geometry mainly depends on the process requirement; one can sacrifice either of heat transfer or pressure loss at the cost of other.

The monograph *Compact Heat Exchangers* by Kays and London [1] remains one of the earliest and the most authoritative sources of experimental j and f data on plate fin surfaces . Although nearly two decades have passed after the latest edition, there has not been any significant addition to this database in open literature. After that several attempts have been made towards the numerical prediction of heat transfer coefficient and friction factor; but they have generally been unable to match experimental data. Several empirical correlations, which have been generated from the data of Kays and London, have found extensive application in industry, particularly in less-critical designs. For critical applications, direct experimental determination of j and f factors for each fin geometry remains the only choice.

In a plate fin heat exchanger the common range of Reynolds number is 500 to 3000 for most of the applications. The Reynolds number is kept low because the hydraulic diameter of the flow passages is generally small due to closely spaced fins and in such conditions operation with low density gases leads to excessive pressure drop unless the gas velocity in the flow passage is kept low.

1.4 Objectives of the study

The main objective of the present work is to evaluate the performance parameters of a counter flow plate fin heat exchanger through hot testing, which includes-

1. Design and fabrication of the test rig for plate fin heat exchanger.
2. To determine the thermal performance parameters like overall heat transfer coefficient, effectiveness and pressure drop of plate fin heat exchanger through hot testing under balanced flow condition.

3. To compare the experimentally obtained values of effectiveness, overall heat transfer coefficient with the values that are obtained from various correlations.

1.5 Organization of the Thesis

This thesis contains six chapters including references

Chapter 1 deals with the general introduction of the compact plate fin heat exchanger and the scope of the future work.

In Chapter 2, a brief literature review on the topics related to the present work has been reported, where emphasis has been laid on the literatures related to the prediction of j and f factors and the thermal performance testing of heat exchangers.

A detailed description of the experimental setup has been given in Chapter 3. The design and fabrication of experimental test rig and instrumentation are discussed in this chapter.

The basic steps involved in Rating, which is used for the calculation of performance parameters of plate fin heat exchanger with offset strip fin geometry, like effectiveness, overall heat transfer coefficient of an already designed heat exchanger is discussed in detail in Chapter 4.

In Chapter 5, the experimental results and detailed procedure for computing the performance parameters of the heat exchanger in balanced condition are presented.

Finally the Chapter 6 is devoted for the concluding remarks and scope for future work.

CHAPTER 2

Literature Survey

LITERATURE SURVEY

Heat exchangers constitute the most important components of many industrial processes and equipment's covering a wide range of engineering applications. Increasing awareness for the effective utilization of energy resources, minimizing operating cost and maintenance free operation have led to the development of efficient heat exchangers like compact heat exchangers. R.K Shah[15] in his elaborate discussion over the classification of heat exchangers has defined the "compact heat exchangers" as one having a surface area density of more than $700 \text{ m}^2/\text{m}^3$. Such compactness is achieved by providing the extended surfaces i.e. fin on the flow passages which work as the secondary heat transfer area.

The main purpose of a recuperative heat exchanger is to facilitate the effective exchange of thermal energy between the two fluids flowing on the either side of a solid portioning wall, during which both the streams experience some viscous resistance and led to pressure drop. So in any heat exchanger the information regarding the quantity oh heat transfer and pressure drop are of utmost importance. Heat transfer and pressure drop characteristics of heat exchanger are mainly expressed in terms of j and f factor respectively.

A large amount of study has been conducted to analyze the heat transfer and pressure drop characteristics of compact heat exchangers in the past few decades. But this study mainly focuses on the OSFs type of plate fin heat exchanger. And therefore the emphasis has been given on the literatures related to the prediction of j and f factors and the thermal performance testing of heat exchangers.

Patankar and Prakash [1] presented a two dimensional analysis for the flow and heat transfer in an interrupted plate passage which is an idealization of the OSFs heat exchanger. The main aim of the study is investigating the effect of plate thickness in a non-dimensional form t/H on heat transfer and pressure drop in OSF channels because the impingement region resulting from thick plate on the leading edge and recirculating region behind the trailing edge are absent if the plate thickness is neglected. Their calculation method was based on the periodically fully developed flow through one periodic module since the flow in OSF channels attains a periodic fully developed behaviour after a short entrance region, which may extend to about 5 (at the most 10) ranks of plates (Sparrow, et al. 1977). Steady and laminar flow was assumed by them between Reynolds numbers 100 to 2000. They found the flow to be mainly laminar in this range,

although in some cases just before the Reynolds no. 2000 there was a transition from laminar to turbulence. Especially for the higher values of t/H . They used the constant heat flow boundary condition with each row of fins at fixed temperature. They made there analysis for different fin thickness ratios $t/H= 0, 0.1, 0.2, 0.3$ for the same fin length $L/H = 1$, and they fixed the Prandtl number of fluid = 0.7. For proper validation they compared there numerical results with the experimental results of [London and Shah] for offset strip fin heat exchangers. The result indicate reasonable agreement for the f factors, but the predicted j factor are twice as large as the experimental data. They concluded that the thick [plate situation leads to significantly higher pressure drop while the heat transfer does not sufficiently improve despite the increased surface area and increased mean velocity.

Joshi and Webb [2] developed an analytical model to predict the heat transfer coefficient and the friction factor of the offset strip fin surface geometry. To study the transition from laminar to turbulent flow they conducted the flow visualization experiments and an equation based on the conditions in wake was developed.

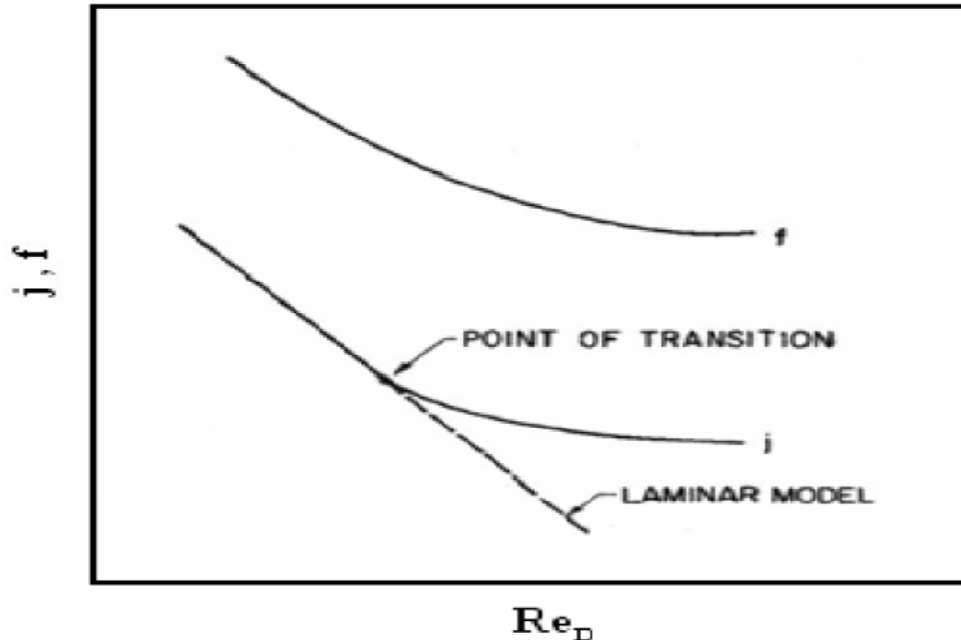


Fig. 2.1 typical j and f characteristics

They also modified the correlations of Weiting [17]. There was some difference between there correlation.

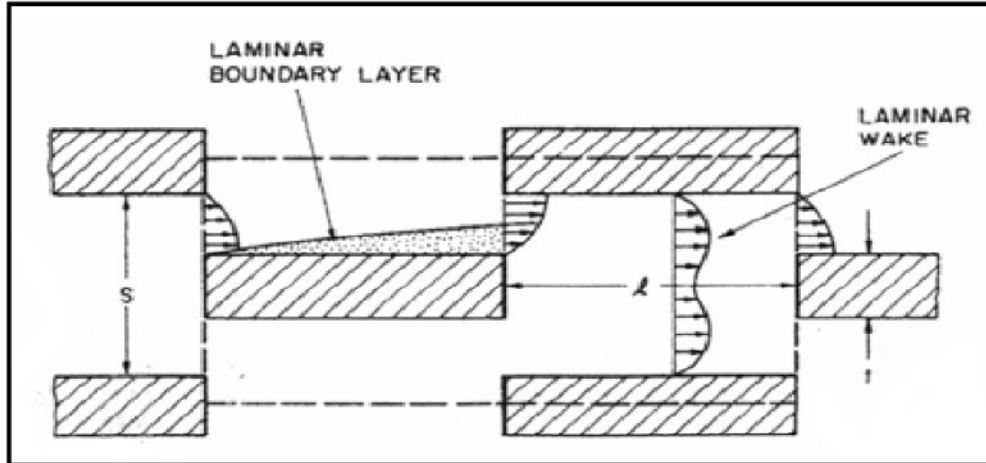


Fig 2.2 Laminar flow on the fins and in the wakes
(Source Joshi and Webb 1987)

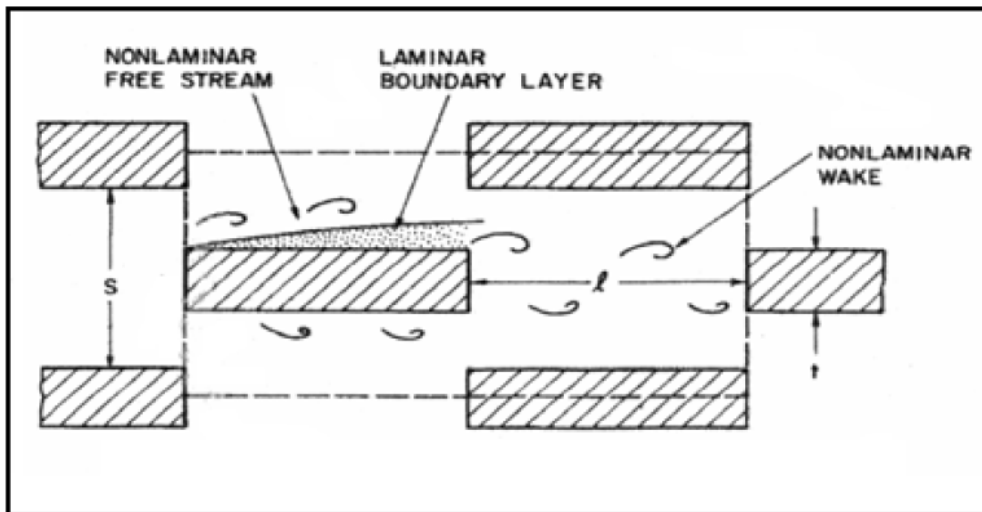


Fig. 2.3 Laminar flow on the fins and oscillating flow on the wakes
(Source Joshi and Webb 1987)

Four different flow regimes (Figure. 2.2 and 2.3) were identified by Joshi and Webb [2] from their experiment. The flow was found to be laminar and steady in the first regime. In the second regime the oscillating flow structures were found in the transverse direction. The flow oscillated in the wake region between two successive fins in the third regime. And in the fourth regime the effect of vortex shedding came into picture. The laminar flow correlation of Joshi and Webb started to under predict the j and f factors at the second regime. So they assumed the Reynolds number at that point as the critical Reynolds number to identify the transition from laminar to turbulent.

Suzuki et al [3] in order to study the thermal performance of a staggered array of vertical flat plates at low Reynolds number has taken a different numerical approach by solving the elliptic differential equations governing the flow of momentum and energy. The validation of their numerical model has been done by carrying out experiments on a two dimensional system, followed by those on a practical offset strip fin heat exchanger. The experimental result was in good agreement with the performance study for the practical offset-strip-fin type heat exchanger in the range of Reynolds number of $Re < 800$.

Tinaut et al [4] developed two correlations for heat transfer and flow friction coefficients for OSFs and plane parallel plates. The working fluid for OSF was engine oil and water was taken for analyzing the parallel plate channels. By using the correlations of Dittus and Boelter and some expressions of Kays and Crawford they obtained their correlations. For the validation of their results they compared their correlations with correlations of Weintg [17]. Although there were some differences between the results but their correlations have been found acceptable upon comparing their results to the data obtained from other correlations.

Manglik and Bergles[5] carried an experimental research on OSFs. They investigated the effects of fin geometries as non dimensional forms on heat transfer and pressure drop, for their study they used 18 different OSFs. After their analysis they arrived upon two correlations, one for heat transfer and another one for pressure drop. The correlations were developed for all the three regions. They compared their results from the data obtained by other researchers in the deep laminar and fully turbulent regions. Their correlations can be acceptable when comparing the results of the expressions to the experimental data obtained by Kays and London [16].

Hu and Herold [6] presented two papers to show the effect of Prandtl no. on heat transfer and pressure drop in OSF array. Experimental study was carried out in the first paper to study the effect for which they used the seven OSFs having different geometries and three working fluids with different Prandtl number. At the same time the effect of changing the Prandtl number of fluid with temperature was also investigated. The study was carried out in the range of Reynolds number varying from 10 to 2000 in both the papers. The results of the two studies showed that the Prandtl number has a significant effect on heat transfer in OSF channel. Although there is no effect on the pressure drop.

Zhang et al [7] investigated the mechanisms for heat transfer enhancement in parallel plate fin heat exchangers including the inline and staggered arrays of OSFs. They have also taken

into account the effect of fin thickness and the time dependent flow behavior due to the vortex shedding by solving the unsteady momentum and energy equation. The effect of vortices which are generated at the leading edge of the fins and travel downstream along the fin surface was also studied. From there study they found that only the surface interruptions increase the heat transfer because they cause the boundary layers to start periodically on fin surfaces and reduce the thermal resistance to transfer heat between the fin surfaces and fluid. However after a critical Reynolds number the flow becomes unsteady and in this regime the vortices play a major role to increase the heat transfer by bringing the fresh fluids continuously from the main stream towards the fin surface.

Dejong et al [8] carried out an experimental and numerical study for understanding the flow and heat transfer in OSFs. In the study the pressure drop, local Nusselt number, average heat transfer and skin friction coefficient on fin surface, instantaneous flow structures and local time averaged velocity profiles in OSF channel were investigated. They compared there results with the experimental results obtained by Dejong and Jacobi [1997] and unsteady numerical simulation of Zhang et al [1997]. There results indicate that the boundary layer development, flow separation and reattachment, wake formation and vortex shedding play an important role in the OSF geometry.

H. Bhowmik and Kwan-Soo Lee [9] studied the heat transfer and pressure drop characteristics of an offset strip fin heat exchanger. For their study they used a steady state three dimensional numerical model. They have taken water as the heat transfer medium, and the Reynolds number (Re) in the range of 10 to 3500. Variations in the Fanning friction factor f and the Colburn heat transfer j relative to Reynolds number were observed. General correlations for the f and j factors were derived by them which could be used to analyze fluid flow and heat transfer Characteristics of offset strip fins in the laminar, transition, and turbulent regions of the flow.

Saidi and Sudden [10] carried out a numerical analysis of the instantaneous flow and heat transfer for OSF geometries in self-sustained time-dependent oscillatory flow. The effect of vortices over the fin surfaces on heat transfer was studied at intermediate Reynolds numbers where the flow remains laminar, but unsteadiness and vortex shedding tends to dominate. They compared there numerical results with previous numerical and experimental data done by Dejong, et al. (1998).

From the studies of few researchers like Patankar and Prakash [1], Kays and London [16] it is easy to get information regarding the effects of OSFs on heat transfer and pressure drop. But most of the researchers have not taken into account the effect of manufacturing irregularities such as burred edges, bonding imperfections, separating plate roughness which also affect the heat transfer and flow friction characteristics on the heat exchanger. Dong et al [11] made experiments and analysis considering the above factors to get better thermal and hydraulic performance from the OSFs. Sixteen types of OSFs and flat tube heat exchangers were used to make the experimental studies on heat transfer and pressure drop characteristics. A number of tests were made by changing the various fin parameters and all the tests were carried out in specific region of air side Reynolds number (500- 7500), at a constant water flow rate. The thermal performance data were analyzed using the effectiveness-NTU method in order to obtain the heat transfer coefficient. They also derived the j factor and f factor by using regression analysis. Results showed that the heat transfer coefficient and pressure drop reduce with enlarging the fin space, fin height and fin length.

Michna et al [12] investigated the effect of increasing Reynolds number on the performance of OSFs. He conducted the experiment at Reynolds number between 5000 to 120000 and found that both heat transfer and pressure drop increased with increasing Reynolds number, because the effect of vortex shedding and eddy formation at turbulent regime. Operation of OSF heat exchangers under these Reynolds number may be useful in systems where minimizing the heat exchanger size or maximizing the heat transfer coefficient is more important than minimizing the pressure drop.

Various experiments are carried out in order to find out the j and f factors of the various heat exchangers and are called as the thermal performance testing. These testing are needed for heat exchangers, which do not have reported j and f data. Therefore, this test is conducted for any new development or modification of the finned surfaces. T. Lestina & K. Bell, Advances in Heat Transfer, told for heat exchangers already existing in the plants this test is done for the following reasons:

- a) Comparison of the measured performance with specification or manufacturing design rating data.
- b) Evaluation of the cause of degradation or malfunctioning.
- c) Assessment of process improvements such as those due to enhancement or heat exchanger

replacement.

Another reason for developing these correlations is that, generally in most heat exchanger problems the working fluid, the heat flow rate and mass flow rate are usually known, so if certain correlations between geometry and fin performance is also known, then the problem can be greatly simplified. For that purpose developing the correlations for fanning friction factor f and Colbourn factor j are important for heat exchanger. Some of the correlations and their investigators are given in Table 2.1. Generally the correlations include three distinct non-dimensional ratios depending on OSF geometry. These are the ratio of free flow area ($\alpha = s/h$), the ratio of heat transfer area ($\beta = t/l$), and the ratio of fin density ($\gamma = t/s$).

Table 2.1 Chronological listing of the correlations for OSF channels

Investigators	Correlation
Manson	$j = \begin{cases} [0.6(1/D_h)^{0.5} Re^{0.5}], & 1/D_h \leq 3.5 \\ [0.321Re^{0.5}], & 1/D_h > 3.5 \end{cases}$ <p style="text-align: center;"><u>For Re<3500:</u></p> $f = \begin{cases} [11.8(1/D_h) Re^{0.67}], & 1/D_h \leq 3.5 \\ [3.371Re^{0.67}], & 1/D_h > 3.5 \end{cases}$ <p style="text-align: center;"><u>For Re>3500:</u></p> $f = \begin{cases} [11.8(1/D_h) Re^{0.67}], & 1/D_h \leq 3.5 \\ [3.371Re^{0.67}], & 1/D_h > 3.5 \end{cases}$ <p style="text-align: center;">Where $D_h = 2sh/(s + h)$</p>
Keys	$j = 0.665Re_1^{-0.5}$ $f = 0.44(t/l) + 1.328Re_1^{-0.5}$
	<p style="text-align: center;"><u>Re<1000:</u></p> $j = 0.483(1/D_h)^{-0.162} \alpha^{-0.184} Re^{-0.536}$

Wieting

$$f = 7.661(1/D_h)^{-0.384}\alpha^{-0.092}Re^{-0.712}$$

Re>2000:

$$j = 0.242(1/D_h)^{-0.322}(t/D_h)^{-0.089}Re^{-0.368}$$

$$f = 1.136(1/D_h)^{-0.781}(t/D_h)^{-0.534}Re^{-0.198}$$

$$\text{Where } D_h = 2sh/(s + h)$$

Re < Re*

$$j = 0.53Re^{-0.5}(1/D_h)^{-0.15}\alpha^{-0.14}$$

$$f = 8.12Re^{-0.74}(1/D_h)^{-0.41}\alpha^{-0.02}$$

Re > Re*+1000

$$j = 0.21Re^{-0.4}(1/D_h)^{-0.24}(t/D_h)^{-0.02}$$

$$f = 1.12Re^{-0.36}(1/D_h)^{-0.781}(t/D_h)^{-0.17}$$

$$\text{Where } D_h = 2(s - t)h / \left[(s + h) + \frac{th}{l} \right]$$

$$Re^* = 257 \left(\frac{l}{s} \right)^{1.23} \left(\frac{t}{l} \right)^{0.58} D_h \left[t + 1.328 \left(\frac{Re}{lD_h} \right)^{-0.5} \right]^{-1}$$

Joshi and Webb:

Re<2000:

$$j = 1.37(I/D_h)^{-0.25}\alpha^{-0.184}Re^{-0.67}$$

$$f = 5.55(I/D_h)^{-0.32}\alpha^{-0.092}Re^{-0.67}$$

Mochizuki et al.

Re>2000:

$$j = 1.17(I/D_h + 3.75)^{-t}(t/D_h)^{0.089}Re^{-0.36}$$

$$f = 0.83(I/D_h + 0.33)^{-0.5}(t/D_h)^{0.534}Re^{-0.20}$$

$$\text{Where } D_h = 2sh/(s + h)$$

$$j = 0.6522Re^{-0.5403}(\alpha)^{-0.1541}\delta^{-0.1499}\gamma^{-0.0678}$$

$$X[1 + 5.269 \times 10^{-5} Re^{1.340} \alpha^{0.504} \delta^{0.456} \gamma^{-1.055}]^{0.1}$$

Manglik and Bergles

$$f = 9.6243Re^{-0.7422}(\alpha)^{-0.1856}\delta^{-0.3053}\gamma^{-0.2659}$$

$$X[1 + 7.669 \times 10^{-8} Re^{4.429} \alpha^{0.920} \delta^{3.7676} \gamma^{0.236}]^{0.1}$$

$$\text{Where } D_h = 4shl/2[(sl + hl + th) + ts]$$

The plate fin heat exchangers find a variety of applications in the field of cryogenics, where high heat transfer performance and high effectiveness are the foremost requirement. But there are many factors which affect their performance, like flow maldistribution, heat in leak from the atmosphere and wall longitudinal heat conduction. Prabhat Gupta, M.D. Atrey [13], have evaluated the performance of a counter-flow heat exchangers for low temperature applications by considering the effect of heat in leak and longitudinal conduction. They developed a numerical model considering the effect of heat in leak and the longitudinal wall heat conduction and made predictions which were compared with the experimental results to understand the quantitative effect of heat in leak and axial conduction parameters on degradation of heat exchanger performance. From there study it was found that in addition to operating and design parameters, the thermal performance of these heat exchangers is strongly governed by various losses such as longitudinal conduction through wall, heat in leak from surrounding, and flow maldistribution, etc.

Randall F Barron, Cryogenic heat exchanger [14], has showed the effect of longitudinal wall heat conduction on the performance of cryogenic heat exchangers. Cryogenic heat exchangers operate at low temperatures where the longitudinal wall heat conduction results in serious performance deterioration these is because they have small distances (on the order of 100 to 200 mm or 4 to 8 in) between the warm and cold ends i.e. they have short conduction lengths. Because of the inherent requirement of high effectiveness for cryogenic heat exchangers, the NTU values are usually large (as high as 500 to 1000), so the effect of longitudinal conduction is most pronounced for heat exchangers having short conduction lengths and large NTU. The wall longitudinal heat conduction reduces the local temperature difference between the two streams, thereby reducing the heat exchanger effectiveness and the heat transfer rate.

CHAPTER 3

Experimental Setup and Procedure

EXPERIMENTAL SETUP AND PROCEDURE

3.1 Detailed Description of various Equipment's and Instruments used

3.1.1 Plate fin heat exchanger

The test section consists of a counter flow plate fin heat exchanger with offset strip fin geometry. This Plate Fin Heat Exchanger was sent here for its performance analysis and to establish the correlation for j and f factors, which is manufactured by APOLLO heat exchangers Mumbai, for BARC Mumbai. Figure 3.3 shows the plate fin heat exchanger with all its dimensions and arrangements of Inlet and Outlet ports. This plate fin heat exchanger consists of offset strip fins. And table 3.1 and 3.2 provides the details of core dimensions and thermal data respectively. This Project is basically an experimental set-up, which is build up for the thermal performance testing of the plate fin heat exchanger for studying its performance. The procured heat exchanger is an Aluminum Plate Fin Heat Exchanger and which was manufactured at Apollo Heat exchangers For BARC Mumbai. As per the information gathered from the BARC Mumbai this heat exchanger is designed for operating at high pressure and is to be used for low temperature applications. The properties such as effectiveness, NTU, overall heat transfer coefficient, colburn factor j and skin friction co-efficient f etc are calculated in order to measure its performance.

Table 3.1(a) Dimensions of procured plate fin heat exchanger.

CORE DATA

	INTERNAL (HOT SIDE)	EXTERNAL (COLD SIDE)
FIN	OSF	OSF
NO. OF PASSAGE	4	5
NO. OF PASS	1	1
FLOW RATE	COUNTER FLOW	COUNTER FLOW

Table 3.1(b) Dimensions of procured plate fin heat exchanger

CORE SIZE

FLOW LENGTH/EFFECTIVE FLOW LENGTH	1000mm/900mm
TOTAL HEIGHT	105mm
TOTAL WIDTH/EFFECTIVE WIDTH	85mm/73mm

Table 3.2 Procured design data of plate fin heat exchanger

THERMAL DATA

HEAT LOAD	5.5 KW	
	HOT SIDE	COLD SIDE
FLUID	HELIUM (HP)	HELIUM (LP)
FLOW RATE	5 g/s	4.8 g/s
INLET TEMP.	36.65 °C	-189.45 °C
OUTLET TEMP.	-177.25 °C	24.39 °C
PRESSURE DROP	0.003 kg/cm ²	0.02 kg/cm ²
OPERATING PRESSURE	7.35 kg/cm ²	7.05 kg/cm ²

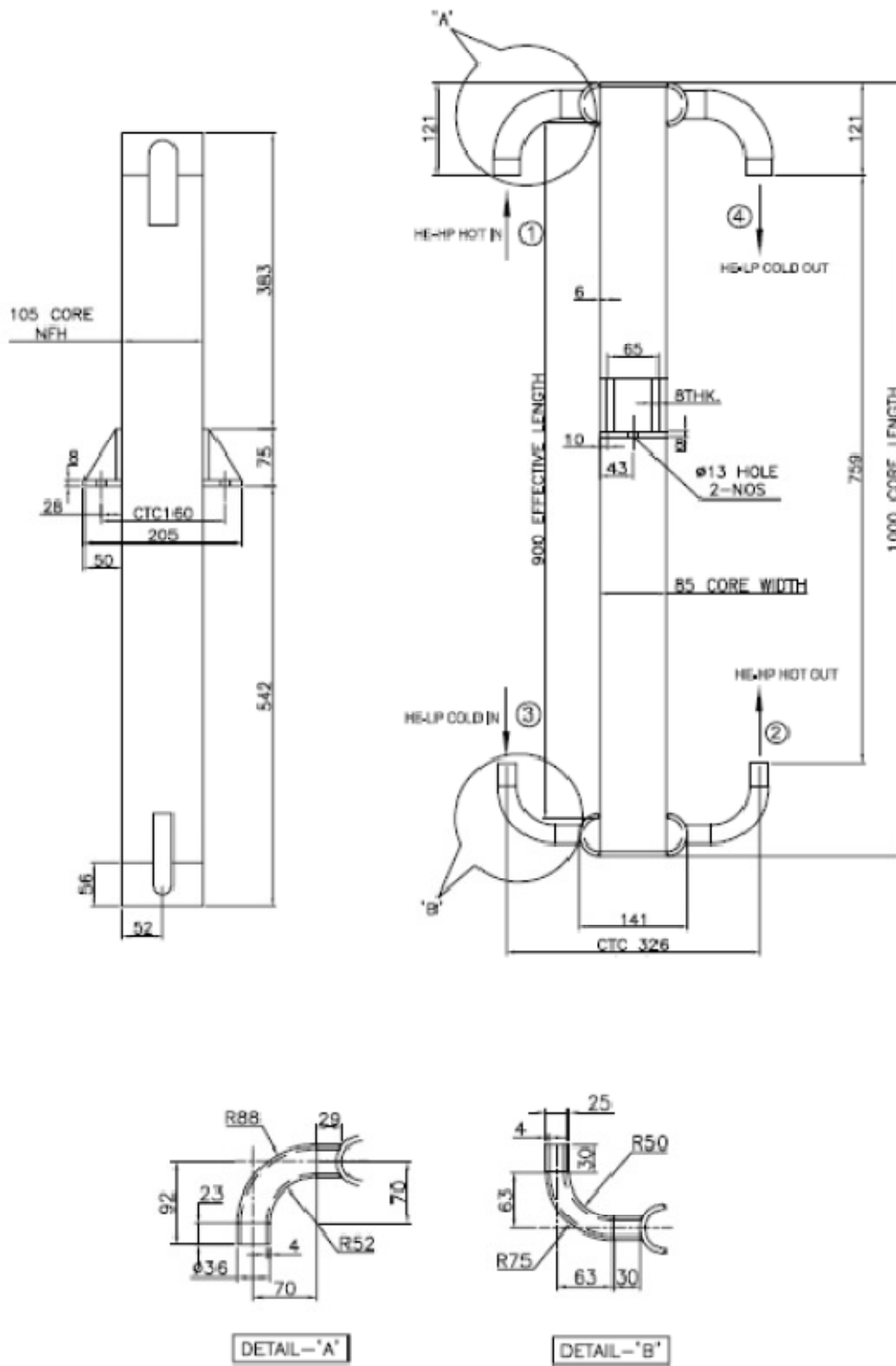
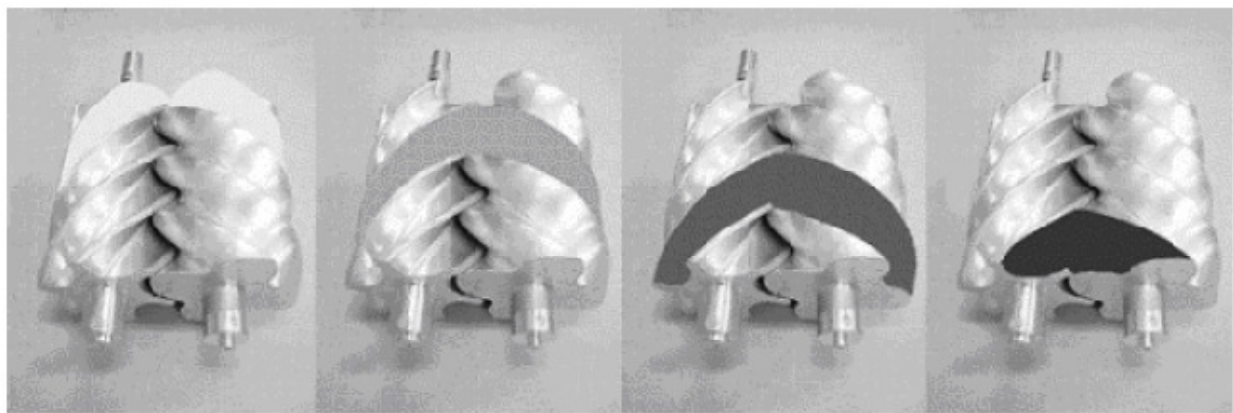


Fig. 3.1 Manufacturing details of Plate fin heat exchanger

3.1.2 Twin – Screw Compressor

Our air supply system consists of a Twin screw rotary compressor which is a positive displacement machine that uses two helical screws known as rotors to compress the gas. The rotors comprise of helical lobes affixed to a front and rear shaft. One rotor is called the male rotor and it will typically have three bulbous lobes. The other rotor is the female rotor and this has valleys machined into it that matches the curvature of the male lobes. Typically the female rotor has five valleys. In a dry running rotary screw compressor, timing gears ensure that the male and female rotors maintain precise alignment. In oil flooded rotary compressor lubricating oils bridges the space between the rotors, both providing a hydraulic seal and transferring mechanical energy between the driving and driven rotors. Gas enters at the suction side and moves through the threads as the screws rotate. The meshing rotors force the gas through the compressor and the gas exits at the end of the screw. A 3-5 rotor combination is provided in the compressor so that, the male rotor turns 1.66 times to every one time of the female rotor. Screw compressors have relatively high rotational speed compared to other types of positive displacement machines which make them compact. They have the ability to maintain high efficiencies over a wide range of operating pressure and flow rates and have long service life and high reliability. All these things make them widely acceptable by various industries of the world.



(a) Suction (b) Entrapment (c) Compression (d) Discharge

Fig. 3.2 working mechanism of Twin Screw Compressor

The twin-screw compressor has been purchased from KAESER KOMPRESSOREN GmBh. The Compressor specification is given below:

Make:	Kaeser (Germany)
Model:	BSD 72
Profile of screw:	Sigma
Free air delivery:	336 m ³ /hr
Suction pressure:	Atmospheric
Maximum Pressure:	11 bar
Operating temperature:	75-1000c
Motor:	37kw, 74amps, 3Φ, 50Hz, 415V±10%, 3000rpm
Oil capacity:	24 L
Cooling:	Air

3.1.3 Heating Element

This heating element was fully designed and developed in our cryogenics lab the location of the heater is as shown in the P&I diagram. It is basically having a shell and tube type of configuration in which incoming cold side fluid i.e. air enters the equipment and leaves the heater through the series of baffles. Our heater contains seventeen number of aluminium baffles through which a five set of heating tube passes. Load of heater is 1575 W, power source 220/230 V, single phase 50Hz AC Supply.

3.1.4 Resistance Temperature Detectors (RTDs)

Resistance thermometers also called as resistance temperature detectors (RTD's) or resistive thermal devices are temperature sensors that exploit, the predictable change in electrical resistance of some materials with changing temperature. It is a positive coefficient device, which means that the resistance increases with temperature. So the material whose resistance increases with temperature is used for making the RTD's. Typical elements used for RTD's include nickel (Ni), copper (Cu), but platinum (Pt) is by far the most common, because it has the best accuracy and stability in comparison to other RTD materials. For it the resistance versus temperature curve is fairly linear and the temperature range is widest and has a very high resistivity, which means that only a small of platinum is required to fabricate a sensor and making platinum costs competitive with other RTD materials. The RTD's are slowly replacing the use of thermocouples in many industrial applications below 600⁰C, due to higher accuracy and reliability.

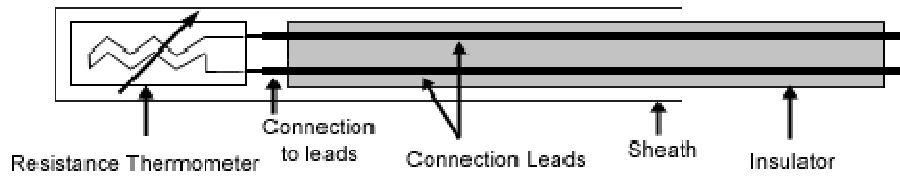


Fig. 3.3 RTD's construction

Figure 3.3 shows the construction of a RTD. RTDs are constructed by one of two different manufacturing configurations. First one is the wire wound RTD which are constructed by winding a thin wire into a coil. Thin film element is a more common configuration, which consists of a very thin layer of metal laid out on a plastic or ceramic substrate. Thin-film elements are cheaper and more widely available because they can achieve higher nominal resistances with less platinum. In order to protect the RTD, a metal sheath encloses the RTD element and lead wires are connected to it. RTD's are available with three different lead wire configurations. The selection of a particular configuration depends on the desired accuracy and instruments to be used for the measurement.

- (a) Two wire configuration
- (b) Three wire configuration and
- (c) Four wire configuration.

RTDs are popular because of their excellent stability and exhibit the most linear signal with respect to temperature when compared to any other electronic temperature sensor. They are generally more expensive than alternatives, however, because of the careful construction and use of platinum. RTDs are also characterized by a slow response time and low sensitivity; and because they require current excitation they can be prone to self heating. And their main limitation is that they cannot be used for measurement of temperature above 660 °C and below -270 °C. Also they are less sensitive to small temperature changes.

RTD's are commonly categorized by their nominal resistance at 0 °C. By far the most common RTD's used in the industry have a nominal resistance of 100 ohms at 0 °C are called as the PT-100 sensors. The relationship between resistance and temperature is very nearly linear and follows the equation.

$$\text{For } < 0 \text{ } ^\circ\text{C} \quad R_T = R_0 [1 + aT + bT^2 + cT^3 (T-100)]$$

$$\text{For } > 0 \text{ } ^\circ\text{C} \quad R_T = R_0 [1 + aT + bT^2]$$

Where,

R_T = resistance at temperature T

R_0 = resistance at nominal temperature

a, b, and c are the constants used to scale the RTD.

We have used four RTD's for the measurement of temperature at the inlet and outlet ports of both hot and cold fluid. And we have done the calibration of RTD's and the calibration chart is and calibration graph are given below.

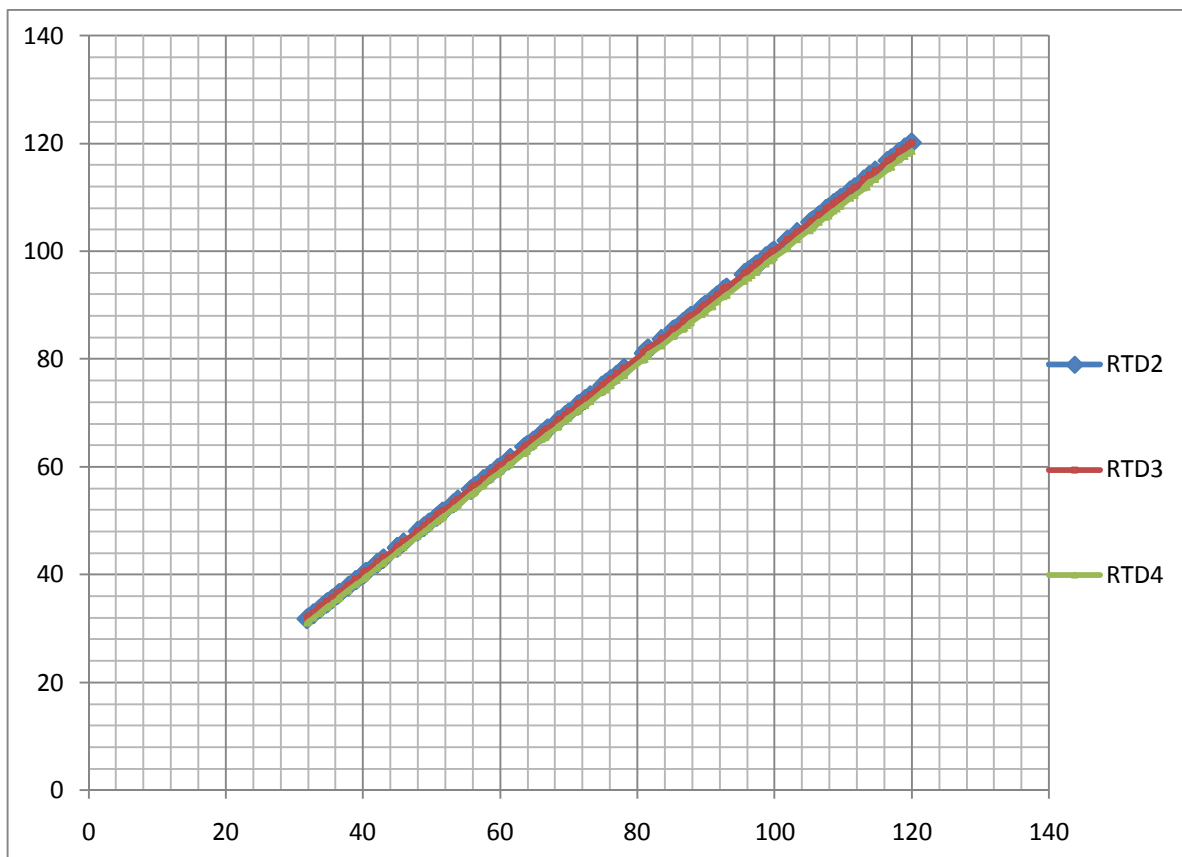


Fig.3.4 RTD Calibration graph

Table 3.3 Calibration Chart

THERMOMETER(⁰ C)	RTD1(⁰ C)	RTD2(⁰ C)	RTD3(⁰ C)	RTD4(⁰ C)
30.5	31.85	31.8	31.98	37.04
32.8	33.67	33.64	33.82	32.84
34	34.87	34.84	35.01	34.03
39	40.31	40.31	40.46	39.48
43.5	44.98	44.98	45.13	44.11
47	48.9	48.89	45.13	44.11
50	51.72	51.69	51.84	50.76
54	55.76	55.74	55.92	54.85
57	58.66	58.7	58.82	59.71
60	61.55	61.6	61.69	60.51
62.8	63.93	63.98	64.07	62.87
65	66.67	66.71	66.78	65.54
68	70.04	70.06	70.24	69.1
71	72.45	72.43	72.63	71.44
74.5	76.1	76.12	76.34	75.12
85	86.69	86.81	86.87	85.57
90	91.64	91.79	91.89	90.64
94.5	96.21	96.34	96.45	95.04
100	101.8	101.91	101.99	100.51
105.5	107.55	107.73	107.77	106.38
107.5	107.9	108.01	108.08	106.55
110.5	113.5	113.36	113.42	111.95
112.5	114.71	114.85	114.89	113.33
115	117.04	117.18	117.22	115.65
117	120	120.07	120.12	118.54

3.1.5 Orifice mass flow meter

A flow meter or flow sensor is an instrument used in almost all mechanical and electrical instrumentation process to measure the flow rate of liquid or gas. An orifice meter is a device used for measuring the rate of fluid flow. Its working is based on the Bernoulli's principle which says that there is a relationship between the pressure of the fluid and the velocity of the fluid. When the velocity increases, the pressure decreases and vice versa. An orifice plate is basically a thin plate with a hole in the middle. It is usually placed in a pipe in which fluid flows. When the fluid flows through the pipe, it has a certain velocity and a certain pressure. When the fluid reaches the orifice plate, with the hole in the middle, the fluid is forced to go through the small

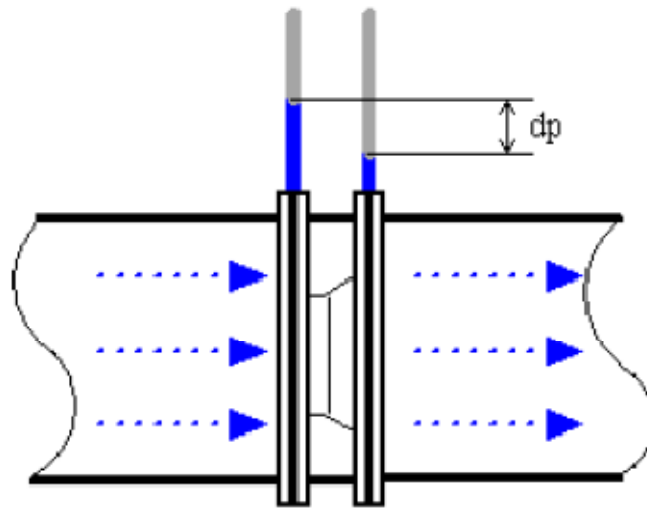


Fig.3.5 Orifice plate

Hole of varying cross section, the point of maximum convergence actually occurs shortly downstream of the physical orifice, and is called as the point of vena contracta(see drawing to the right). Both the velocity and pressure of the fluid changes while it passes through the orifice plate . Beyond the vena contracta, the fluid expands and the velocity and pressure change once again. The volumetric and mass flow rates are obtained from the Bernoulli's equation by measuring the difference in fluid pressure between the normal pipe section and at the vena contracta, shown in fig 3.4. The pressure recovery is limited for an orifice plate and the permanent pressure loss depends primarily on the area ratio. For an area ratio of 0.5, the head loss is about 70 - 75% of the orifice differential.

The mass flow rate can be calculated from the formula given below:

$$Q = CC_d\sqrt{2gH}$$

Where,

Q = mass flow rate

$$C = \text{is area constant} = \frac{A_2}{\sqrt{1 - \left(\frac{A_1}{A_2}\right)^2}}$$

C_d = coefficient of discharge

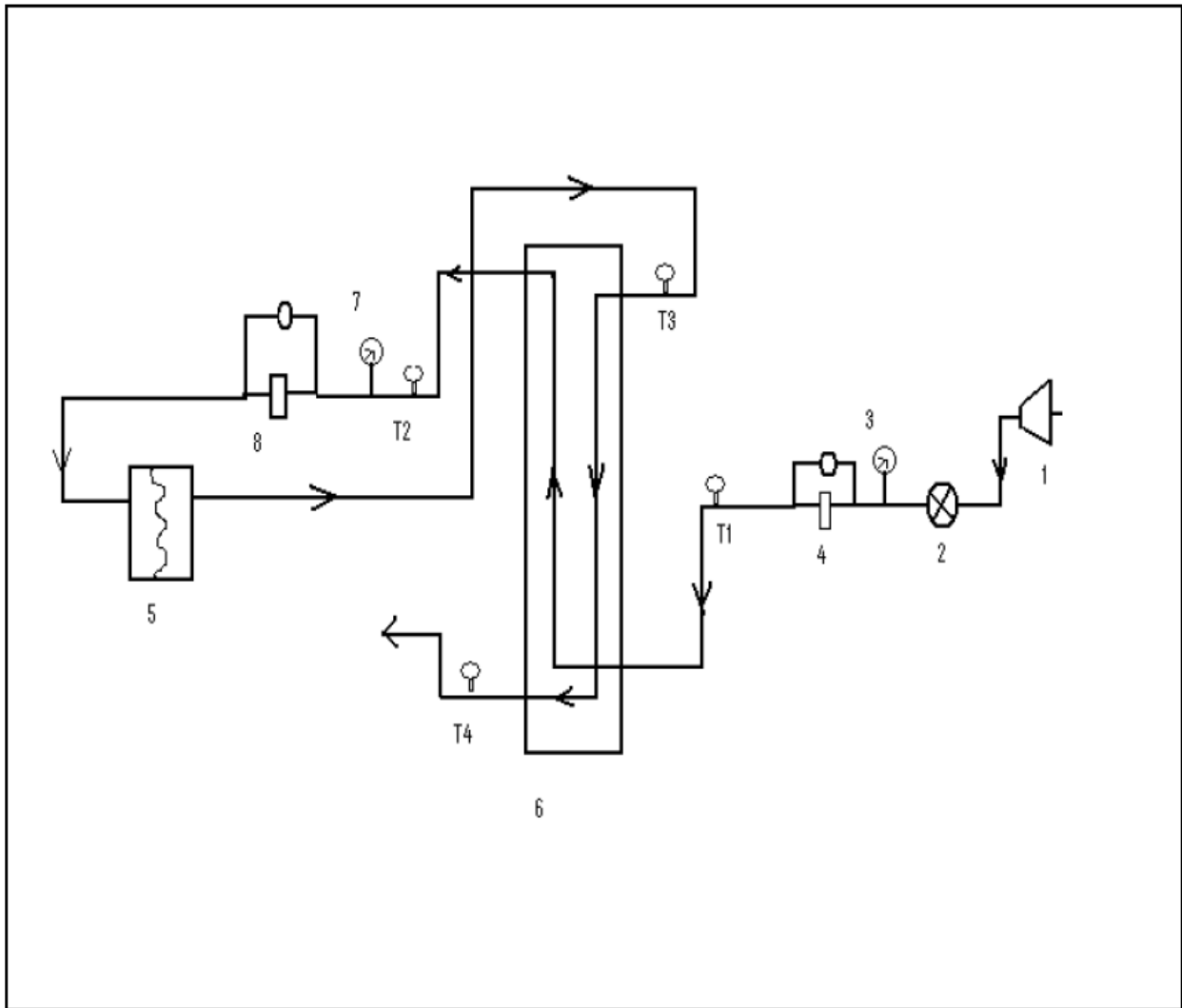
H = head of air

3.1.6 Variac or Autotransformer

Variac also called as an Autotransformer is an electrical transformer with only one winding. The auto prefix refers to the single coil acting on itself rather than any automatic mechanism. In an autotransformer portions of the same winding act as both the primary and secondary. The winding has at least three taps where electrical connections are made. Autotransformers are often used to step up or step down between voltages in the 110-117-120 volt range and voltages in the 220-230-240-volt range. We have used two variacs

An autotransformer has a single winding with two end terminals, and one or more terminals at intermediate tap points. The primary voltage is applied across two of the terminals, and the secondary voltage taken from two terminals, almost always having one terminal in common with the voltage source and electrical load. The primary and secondary circuits therefore have a number of windings turns in common. Since the volts-per-turn is the same in both windings, each develops a voltage in proportion to its number of turns. The other end of the source and load are connected to taps along the winding. Different taps on the winding correspond to different voltages, measured from the common end. In a step-down transformer the source is usually connected across the entire winding while the load is connected by a tap across only a portion of the winding. In a step-up transformer, conversely, the load is attached across the full winding while the source is connected to a tap across a portion of the winding.

3.2 Test Rig



1: Compressor	2: Control Valve	3,7: Pressure Taps
4,8: U- Tube manometer	5: Heater	6:Test section
T ₁ , T ₂ , T ₃ , T ₄ are RTD's		

Fig. 3.6 Schematic P&I diagram of the Experimental Test Rig



Fig.3.7 Photograph of the Experimental Setup

3.2.1 Procedure for Hot Testing

Air is used as the as working fluid in this experiment. The apparatus was connected to a compressor system which is capable of continuously delivering dry air .The compressed air from the compressor enters the laboratory through a control valve which is used to regulate the flow rate through the heat exchanger and then routed to the testing heat exchanger. This is the cold side fluid which is made to enter the heat exchanger from the bottom side and when it comes out it is made to pass through the heater, where it gets heated up and which is then again fed into the heat exchanger from top end and which finally results in hot and cold fluid streams. The heat supplied to the heater is controlled with the help two variacs. The pressure taps are located on the upstream and downstream of heat exchanger to measure the pressure drop across the heat exchanger. These pressure taps was connected with tubing and which is connected to a U-tube manometer to give an average reading of the pressure drop. The air inlet and outlet temperatures at both ends of heat exchanger core were measured using four RTD's. The air flow rate was measured using the Rotameter and the mass flow rate of both the fluids can be measured using orifice meter. The orifice meter is used only when the test is carried out in unbalanced condition i.e. when the mass flow rates on both sides is different. The pressure drop across the orifice plate can be measured by using U-tube manometers.

It was ensured that there is no mass leak from the system. And the test section was carefully insulated, by using glass wool sheets and asbestos tapes to eliminate heat losses from the system to the surrounding. The air flow rate through the test section was set using the control valve, and the temperatures, core pressure drop across the heat exchanger and the room pressures were recorded for flow in the required range. The system was then allowed to run until the steady state is achieved. The system was considered to be at steady state when all the temperature readings steadily decrease and steadily increase for at least one minute. Once the steady state was achieved for a particular mass flow rate the air flow rate and the temperature and pressure differentials of the air stream across the core are accurately measured for estimating the rate of heat transfer, pressure drop and various performance parameters like effectiveness, NTU, and heat transfer coefficient. In experimental calculation in order to take into account the effect of wall longitudinal heat conduction the KROGERES formula was used. For theoretical calculation the usual procedure for rating was followed and the calculations were done in the excel sheet.

CHAPTER 4

Rating Procedure

RATING PROCEDURE

Design of heat exchanger involves two types of problem – (a) Sizing and (b) Rating. Sizing involves the determination or we can say selection of type of heat exchanger, flow arrangement, material of heat exchanger and physical dimensions of the heat exchanger to meet the specified heat transfer and pressure drop requirements. Whereas, Rating of the heat exchanger consists of finding the thermal performance parameters like, effectiveness, heat transfer coefficient and pressure drop of an already designed heat exchanger whose dimensions are known to us. We are working on the rating problem. Since the outlet temperatures are not known for the rating problem, the average fluids mean temperatures have to be projected first. The heat transfer coefficient and the effectiveness of the plate fin heat exchanger are found based on different correlations existing in literature. The outlet temperatures and the average fluid temperatures are calculated from the effectiveness value and then compared with the values assumed earlier. The above procedure is carried out until the calculated values of the mean fluid temperatures matches with the assumed values. Following steps show the detailed rating procedure:

1. The first step in rating procedure is to calculate the various surface geometrical properties of the heat exchanger. We are using a plate fin heat exchanger with offset strip fin geometry, and geometry of the offset strip fin surface is described by the following parameters:

- i) Fin spacing (s), excluding the fin thickness,
- ii) Fin height (h), excluding the fin thickness,
- iii) Fin thickness(t) and,
- iv) Fin strip length(l or L_f)

The lateral fin offset is generally the same and equal to half the fin spacing (including fin thickness). Figure 4.1 shows a schematic view of the rectangular offset strip fin surface and defines the basic geometric parameters. But the present heat exchanger has different fin geometries for the hot and cold side fluids. Table 4.1 shows the fin specifications for hot and cold side of the heat exchanger.

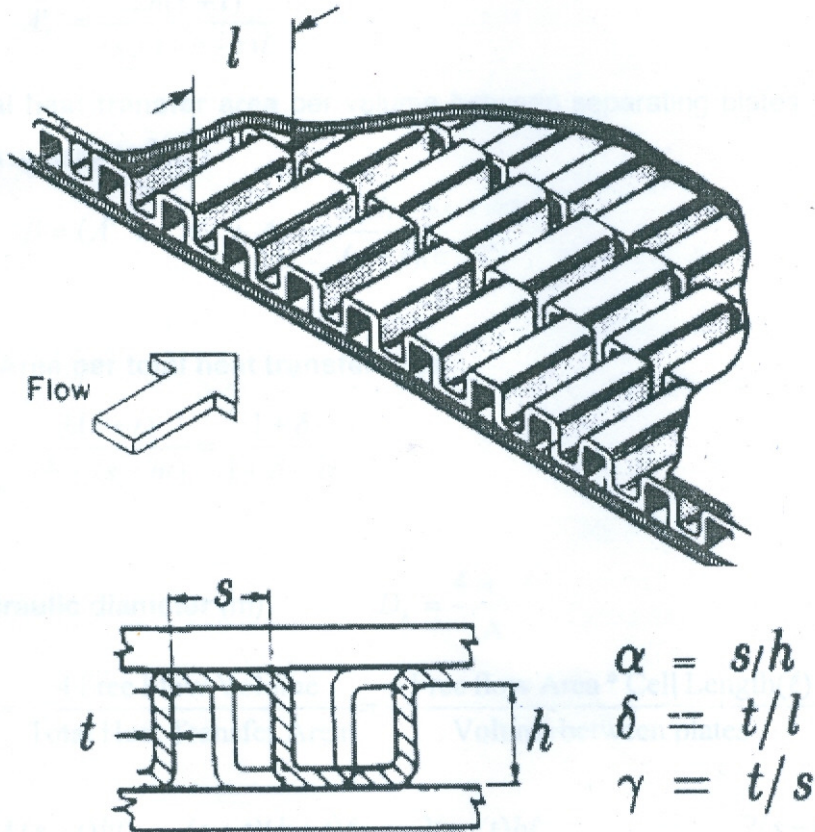


Figure 4.1 Geometry of Typical Offset Strip Fin Surface

Table 4.1 Core Data (fin specifications)

	Hot Fluid	Cold Fluid
No. Of passes (N)	4	5
Fin thickness (t)	0.2mm	0.2mm
Fin frequency (f)	588	714
Fin length (l)	5mm	3mm
Fin height (h)	9.5mm	9.5mm
Plate thickness (a)	0.8mm	0.8mm

There are some secondary geometrical parameters which are derived from the above basic fin geometries, which are calculated as follows. The calculation is done for the hot side fluid and by following the same steps the results can be obtained for cold side.

i) Fin spacing, $s = \frac{(1 - f * t)}{(f)} = 0.001501 \text{ m}$

ii) Free flow area to Frontal area,

$$\sigma = \frac{a_{ff}}{a_{fr}} = \frac{(s - t)h}{(h + t)(s + t)} = \frac{(0.001501 - 0.0002) \times 0.0093}{(0.0093 + 0.0002)(0.001501 + 0.0002)} = .00001615$$

iii) Heat transfer area per fin, a_s

$$a_s = 2hl + 2ht + 2sl = 2 * 0.0093 * 0.005 + 2 * 0.001501 * 0.005 + 2 * 0.0093 * 0.0002 = 0.0001117$$

iv) Ratio of fin area to heat transfer area of fin,

$$\frac{2h(l + t)}{2(hl + sl + ht)} = \frac{2 \times 0.0093(0.005 + 0.0002)}{2(0.0093 \times 0.005 + 0.005 \times 0.001501 + 0.0093 \times 0.0002)} = 0.86565$$

v) Equivalent diameter, $De = \frac{(4 * \text{Freeflowarea} * \text{length})}{\text{heattransferarea}}$

$$= \frac{2(s - t)hl}{hl + sl + ht} = \frac{2(0.001501 - 0.0002) \times 0.0093 \times 0.005}{(0.0093 \times 0.005 + 0.001501 \times 0.005 + 0.0093 \times 0.0002)} = 0.002165810 \text{ m}$$

vi) Distance between plates, $b = h + t = 0.0093 + .0002 = .0095 \text{ m}$

2. Heat transfer area, A

The various heat transfer area for hot side are calculated as follows

i) Total area between plates, $A_{frh} = b \times N_h \times W = 0.0095 \times 4 \times 0.073 = 0.0028$

ii) Total free flow area, $A_{ffh} = \sigma \times A_{frh} = 0.748742226 * 0.0028 = 0.0021 \text{ m}^2$

iii) Wall conduction area, $a_{wh} = A_{frh} - A_{ffh} = 0.0028 - 0.0021 = 0.001213 \text{ m}^2$

iv) Total heat transfer area, $A_h = \frac{4 \times A_{ffh} \times L}{D_e} = \frac{4 \times 0.0021 \times 0.9}{0.002165810} = 3.4524 \text{ m}^2$

v) Total wall conduction area = $a_{wh} + a_{wc} = 0.0007 + 0.001 = 0.0017 \text{ m}^2$

3. Heat exchanger input data

Temperature of hot gas at inlet = 368.81 K

Temperature of cold gas at inlet = 311.93 K

Pressure at inlet of cold gas = 1.21 bar

Pressure of gas at hot inlet = 1.17 bar

Mass flow rate of cold gas = 0.0095 kg/s

Mass flow rate of hot gas = 0.0095 kg/s

4. Estimation of average temperature

Since the fluid outlet temperatures are not known for the rating problem, the average fluids mean temperatures have to be predicted first. The fluid properties at the predicted mean temperatures of 342.02 K and 338.71 K for hot and cold fluid are obtained from property package, Gaspak.

The properties of hot gas at the mean temperature are,

Specific heat, $C_p = 1.04086 \text{ KJ/kgK}$

Viscosity, $\mu = 0.0000198 \text{ Pa-s}$

Prandtl number, $Pr = 0.7169882$

Density, $\rho = 1.14249 \text{ kg/m}^3$

The properties of cold gas at the mean temperature are,

Specific heat, $C_p = 1040.67 \text{ KJ/kgK}$

Viscosity, $\mu = 0.0000192 \text{ Pa-s}$

Prandtl number, $Pr = 0.7167$

Density, $\rho = 1.321 \text{ kg/m}^3$

5. Heat Transfer coefficients and surface effectiveness of fins

The calculations for the heat transfer coefficients for the hot and cold gas are analogous. So the calculations are presented for the hot fluid and can be obtained for cold gas by following the same procedure

i) Core mass velocity, $G = \frac{m}{A_{ffh}} = \frac{0.0095}{0.0021} = 4.5739 \text{ kg/s-m}^2$

ii) The Reynolds no., $Re = \frac{GDe}{\mu} = \frac{4.5379 \times 0.002165810}{0.0000198} = 500.31$

iii) The critical Reynolds number Re^* proposed by Joshi and Webb is

$$\begin{aligned} Re^* &= 257 \left(\frac{l}{s}\right)^{1.23} \left(\frac{t}{l}\right)^{0.58} D_h \left[t + 1.328 \left(\frac{Re}{ID_h}\right)^{-0.5} \right]^{-1} \\ &= 257 \times \left(\frac{0.005}{0.001501}\right)^{1.23} \times \left(\frac{0.0002}{0.005}\right)^{0.58} \times 0.002165 \left[0.0002 + 1.328 \left(\frac{500.310}{0.005 \times 0.002165}\right)^{-0.5} \right]^{-1} \\ &= 956.1409069 \end{aligned}$$

iv) The Colburn factor j for ($Re^* > Re$) is given by correlation proposed by Joshi and Webb is

$$\begin{aligned}
j &= 0.53 \text{Re}^{-0.5} (1/D_h)^{-0.15} \alpha^{-0.14} \\
&= 0.53 \times (500.31)^{-0.5} \times (2.30860463)^{-0.15} \times (0.161397849)^{-0.14} \\
&= 0.02698
\end{aligned}$$

v) The convective heat transfer coefficient is given by

$$h_h = \frac{(j_h * C_h * G_h)}{(\text{Pr})^{0.667}} = \frac{(0.02698 \times 1040.86 \times 4.5739)}{(0.7169882)^{0.667}} = 160.34 \text{ W/m}^2\text{K}$$

vi) The fin parameter is given by

$$M = \sqrt{\frac{(2 * h_h)}{(K_f * t)}} = \sqrt{\frac{(2 \times 160.3430)}{(165 \times 0.0002)}} = 95.5787$$

vii) l_h = Height of fins for hot side= b

And for cold side passages which are the outer layers $l_h = b/2$.

viii) The fin effectiveness is given by

$$n_f = \tanh(Ml_h) / (Ml_h) = 0.93280$$

vi) Overall surface effectiveness is given by

$$\eta_{oh} = 1 - (a_f / a_s) * (1 - \eta_f) = 1 - (0.86565)(1 - 0.93280) = 0.94183$$

Similarly, convective heat transfer coefficient and overall surface effectiveness for cold fluid are

$$h_c = 179.948 \text{ W/m}^2\text{K}, \eta_{oc} = 0.87593 \text{ and } j_c = 0.03536$$

6. Overall heat transfer coefficient and NTU

The overall heat transfer coefficient is given by

$$\frac{1}{(U_o A_o)_h} = \frac{1}{(\eta_{oh} h_h A_h)} + \frac{a}{K_w A_w} + \frac{1}{(\eta_{oc} h_c A_c)}$$

Where,

$$A_w = \text{lateral conduction area} = W \times L \times (2N_p + 2) = 0.073 \times 0.886(2 \times 4 + 2) = 0.657 \text{ m}^2$$

$$\begin{aligned}
\frac{1}{(U_o A_o)_h} &= \frac{1}{(0.94183 \times 160.34 \times 304524)} + \frac{0.0008}{165 \times 0.657} + \frac{1}{(0.87593 \times 179.9486 \times 5.2152)} \\
&= 0.0031419
\end{aligned}$$

$$(U_o A_o)_h = 318.27751 \text{ W/K}$$

$$\text{Overall heat transfer coefficient, } U_{oh} = \frac{(U_o A_o)h}{A_{oh}} = \frac{318.27751}{3.4524} = 92.19027 \text{ W/m}^2\text{K}$$

$$\text{And } U_{oc} = \frac{(U_o A_o)_c}{A_{oc}} = \frac{318.2775}{5.452} = 61.0288$$

$$\text{Number of transfer units, } N_{tu} = \frac{U_o A_o}{C_{\min}} = \frac{318.27751}{9.8876} = 32.18956$$

7. Effectiveness of heat exchanger without considering the effect of longitudinal conduction

$$\varepsilon = \frac{1 - e^{-N_{tu}(1-C_r)}}{1 - C_r e^{-N_{tu}(1-C_r)}} = \frac{1 - e^{-32.18956(1-0.9999)}}{1 - 0.9999 e^{-32.18956(1-0.9999)}} = 0.96989$$

8. Effect of wall longitudinal heat conduction

The consequence of longitudinal heat conduction is to decrease the effectiveness of heat exchanger. The decrease in the effectiveness of heat exchanger is found out by using the Kroeger's equation.

i) Wall conduction area, $a_w = 0.0017 \text{ m}^2$

ii) Conductivity of fin, $K_w = 165 \text{ W/m}^2\text{K}$

iii) Wall conduction parameter, $\lambda = \frac{K_w a_w}{LC_{\min}} = \frac{165 \times 0.0017}{0.9 \times 9.8876} = 0.03225$

iv) $y = \lambda N_{tu} C_r = 0.03225 \times 32.18956 \times 0.9999 = 1.03795$

v) $\gamma = \frac{(1 - C_r)}{(1 - C_r)(1 + y)} = \frac{(1 - 0.9999)}{(1 - 0.9999)(1 + 1.037955)} = .0000141432$

vi) $\phi = \gamma(y/(1 + y))^{1/2} \left[\frac{(1 + \gamma)y}{1 - \gamma(1 + \gamma)y} \right] = 1.04768 \times 10^{-5}$

vii) $\varphi = \frac{(1 + \phi)}{(1 - \phi)} = \frac{(1 + 1.04768 \times 10^{-5})}{(1 - 1.04768 \times 10^{-5})} = 1.00002$

viii) $r_1 = \frac{(1 - C_r)N_{tu}}{1 + \lambda N_{tu} C_r} = \frac{(1 - 0.9999) \times 32.18956}{1 + 0.032247 \times 32.18956 \times 0.9999} = 0.000910499$

ix) $(1 - \varepsilon) = \frac{(1 - C_r)}{\varphi \exp(r_1) - C_r} = \frac{(1 - 0.9999)}{1.0002 \times \exp(0.000910499) - 0.9999} = 0.0582595$

$$x) \quad \varepsilon = [1 - (1 - \varepsilon)] = 1 - .058254 = 0.94174$$

This is the value of the actual effectiveness of heat exchanger subsequently considering wall longitudinal heat conduction effect. Outlet temperatures of fluids based on this value of effectiveness are found as follows.

The outlet temperature of hot fluid is given by

$$T_{ho} = T_{hi} - \frac{\varepsilon C_{\min} (T_{hi} - T_{ci})}{C_h} = 368.81 - \frac{0.94174 \times 9.8876 (368.81 - 311.93)}{9.88817} = 315.246K$$

The outlet temperature of cold fluid is,

$$T_{co} = T_{ci} + \frac{\varepsilon C_{\min} (T_{hi} - T_{ci})}{C_c} = 311.93 + \frac{0.94174 \times 9.8876 (368.81 - 311.93)}{9.8876} = 365.4964K$$

Mean temperature of hot and cold fluid is given by,

$$\text{Mean temperature of hot fluid is, } T_{hm} = \frac{T_{hi} + T_{ho}}{2} = \frac{368.81 + 315.246}{2} = 342.028K$$

$$\text{Mean temperature of cold fluid is, } T_{cm} = \frac{T_{ci} + T_{co}}{2} = \frac{311.93 + 365.4964}{2} = 338.713K$$

Since our calculated mean temperatures match with the assumed values of mean temperature we can stop the iteration here, otherwise we would have taken the values of mean temperature obtained in the above step and carried out the iteration once again, till the assumed and found values are identical

9. Pressure drop

Since the pressure drop of cold fluid is more critical so the calculation is shown for cold fluid

i) The friction factor (f) for $Re^* > Re$ is given by

$$f = 8.12 Re^{-0.74} (1/D_h)^{-0.41} \alpha^{-0.02} \\ = 0.05999$$

ii) The pressure drop, $\Delta p = \frac{4fLG^2}{2D_e \rho_b} = \frac{4 \times 0.05999 \times 0.9 \times (3.9169)^2}{2 \times 0.001674 \times 1.18351} = 836.0924 \text{ Pa}$

CHAPTER 5

Performance Analysis

PERFORMANCE ANALYSIS

The main aim of present work is to calculate the performance parameters like, effectiveness, overall heat transfer coefficient of the plate fin heat exchanger. In order to find the performance of present heat exchanger a number of experiments were carried out at different mass flow rates and at different hot fluid inlet temperature under balanced flow. Table 5.1 shows the experimentally observed data

Table 5.1 experimentally observed data.

Flow Rate (litr/min)	P ₁ (Kg/cm ²)	P ₂ (Kg/cm ²)	Δh_c (mm of Hg)	Δh_h (mm of Hg)	T ₁ (°C)	T ₂ (°C)	T ₃ (°C)	T ₄ (°C)
300	0.08	0.06	9	6	42.24	87.34	96.2	47.15
400	0.14	0.12	15	12	38.35	87.02	95.12	43.01
500	0.2	0.17	25	22	38.93	88.49	96.12	43.11
550	0.24	0.20	30	26	39.82	88..83	96.66	43.48
588	0.28	0.24	31	27	40.41	88.45	96.20	43.99
650	0.32	0.26	40	35	41.16	87.86	95.95	44.17
300	0.08	0.06	8	6	40.92	62.06	66.48	43.06
400	0.135	0.10	16	14	42.77	62.90	66.43	44.56
500	0.2	0.16	24	22	39.57	62.52	66.02	41.69
600	0.28	0.23	31	30	39.94	62.44	65.98	41.73
650	0.34	0.28	37	34	42.72	62.77	66.34	44.06

5.1 CALCULATIONS:

The temperatures values which are obtained experimentally are first of all corrected using the calibration chart, and also the pressure values are converted in units of Pa or bar, and then used for further calculations.

$T_1 = 38.93^\circ\text{C}$, $T_2 = 87.23^\circ\text{C}$, $T_3 = 95.96^\circ\text{C}$, $T_4 = 48.10^\circ\text{C}$, $P_1 = 1.21 \text{ bar}$, $P_2 = 1.18 \text{ bar}$,

Flow rate = 500 liter/min

$$\begin{aligned} 1. \text{Mass flow rate} &= \text{Volume flow rate} \times \frac{p_4}{RT_4} \\ &= \frac{500 \times 10^{-3}}{60} \times \frac{1.01325 \times 10^5}{287 \times 316.98} = 0.01 \text{ kg/s} \end{aligned}$$

2. Heat capacity of hot and cold fluids,

$$C_c = m_c \cdot C_{pc} = 0.010087 \text{ KW/K}$$

$$\text{for hot fluid, } C_h = m_h \cdot C_{ph} = 0.010093 \text{ KW/K}$$

3. Capacity Rate ratio, $C_r = C_{\min}/C_{\max} = 0.9994$

$$4. \text{Effectiveness, } \varepsilon_h = \frac{C_h(T_{hinlet} - T_{hexit})}{C_{min}(T_{hinlet} - T_{cinlet})} = 91.134$$

$$\varepsilon_c = \frac{C_c(T_{cexit} - T_{cinlet})}{C_c(T_{hinlet} - T_{cinlet})} = 86.920$$

5. Number of transfer units, $NTU = 15.009$

After considering the effect of longitudinal heat conduction. Same steps as described in Chapter 4 are followed, but here the NTU value is assumed in such a way that the effectiveness obtained from Kroger's equation matches with the experimental value of effectiveness.

6. Overall Heat transfer conductance, UA_0

$$\begin{aligned} UA_0 &= NTU \times C_{\min} = 15.009 \times 0.010087 \\ &= 160.898 \text{ W/K} \end{aligned}$$

Here also the surface geometrical properties are calculated by following the procedure as mentioned in Chapter 4. Table 5.2 shows the performance parameters of heat exchanger obtained after calculation.

Table 5.2 Performance of heat exchanger

Flow Rate (lit/min)	Mass flow rate (kg/s)	ε_h	ε_c	NTU	UA ₀ W/K	Re _h	Re _c	ΔT_{HOTEND}	$\Delta T_{COLDEND}$
300	0.0057	89.902	83.749	13.64	80.95	298.67	199.72	8.73	5.87
400	0.0074	90.236	85.90	15.24	117.37	416.04	278.22	7.97	5.53
500	0.0103	91.134	86.920	15.00	160.89	542.44	362.75	7.44	5.05
550	0.0116	92.08	86.365	16.24	196.09	610.9	406.46	7.72	4.53
588	0.0127	92.001	86.247	15.70	207.64	668.83	445	7.64	4.45
650	0.0142	92.786	85.371	17.49	258.57	747.83	497.56	7.98	3.94
300	0.0057	88.108	83.064	11.76	69.74	280.24	186.48	4.3	3.02
400	0.0078	89.937	85.480	13.25	107.60	419.28	277.56	3.36	2.33
500	0.0101	88.48	86.814	9.79	102.89	491.54	399.77	3.48	3.04
600	0.011	90.004	86.597	11.28	135.41	702.63	465.13	3.46	2.58
650	0.014	90.572	85.114	12.00	174.87	789.66	525.48	3.49	2.21

In order to compare our experimental results with the values that are obtained from theoretical correlations, some graphs are plotted for which the experiment is conducted at

different mass flow rates and at two different hot inlet temperatures of 66 and 96°C. Some of the graphs are shown below:

5.2 Variation of Effectiveness with Mass Flow Rate

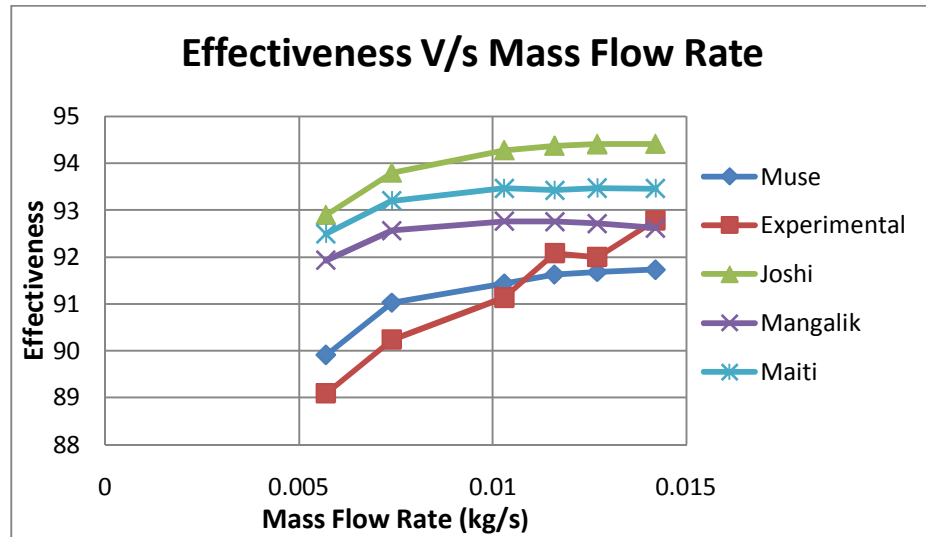


Fig. 5.1 Variation of effectiveness with mass flow rate (hot inlet temperature=96°C)

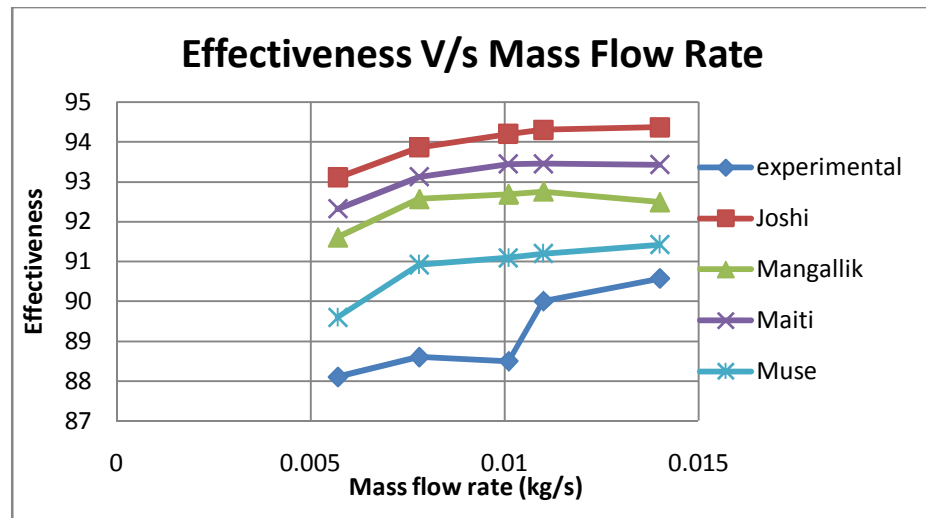


Fig. 5.2 Variation of effectiveness with mass flow rate (hot inlet temperature=66°C)

Figure 5.1 and 5.2 shows the variation of effectiveness obtained experimentally as well as with theoretical correlations and that obtained with simulation software Aspen with mass flow rate. It is seen that in both the cases effectiveness increases with mass flow rate. Experimental hot effectiveness first increases, then becomes almost constant for certain mass flow rates and

then again increases. However from two figures it can be seen that the value of experimental effectiveness is more when hot inlet temperature is 96°C as compared to effectiveness value when hot inlet temperature is 66°C. So it can be concluded that with increase in hot inlet temperature effectiveness increases.

5.3 Variation of Overall thermal Conductance with Mass flow rate

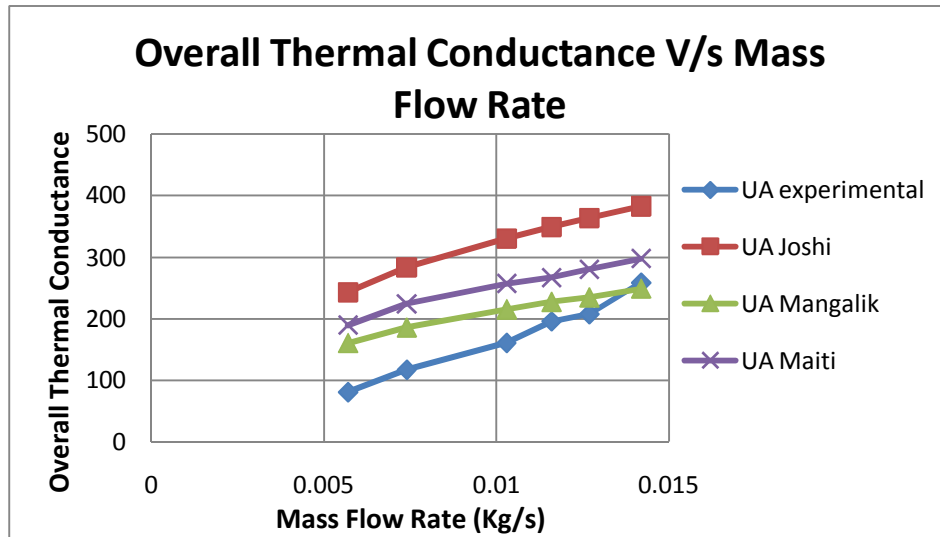


Fig. 5.3 Variation of overall thermal conductance with mass flow rate (hot inlet temperature of 96°C)

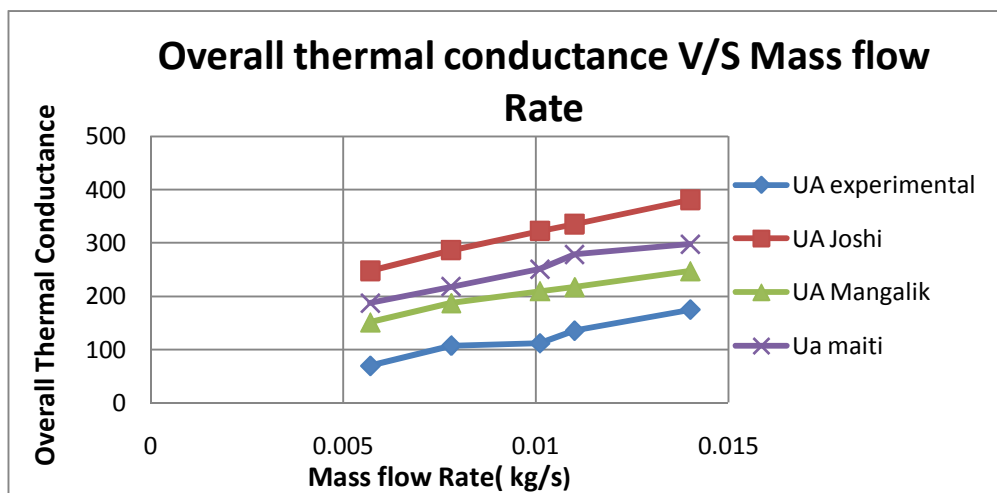


Fig. 5.4 Variation of overall thermal conductance with mass flow rate (hot inlet temperature of 66°C)

Figure 5.3 and 5.4 shows the variation of overall thermal conductance with mass flow rate for hot inlet temperature of 96°C and 66°C respectively. It can be seen that the theoretical as

well as experimental overall heat transfer coefficient increases with increasing mass flow rate. It is due to the fact that with increasing mass flow rate the Reynolds number increases and as a result Colburn factor (j) also increases which is directly proportional to heat transfer coefficient, so overall thermal conductance increases.

5.4 Variation of Hot and Cold Effectiveness with Mass Flow Rate

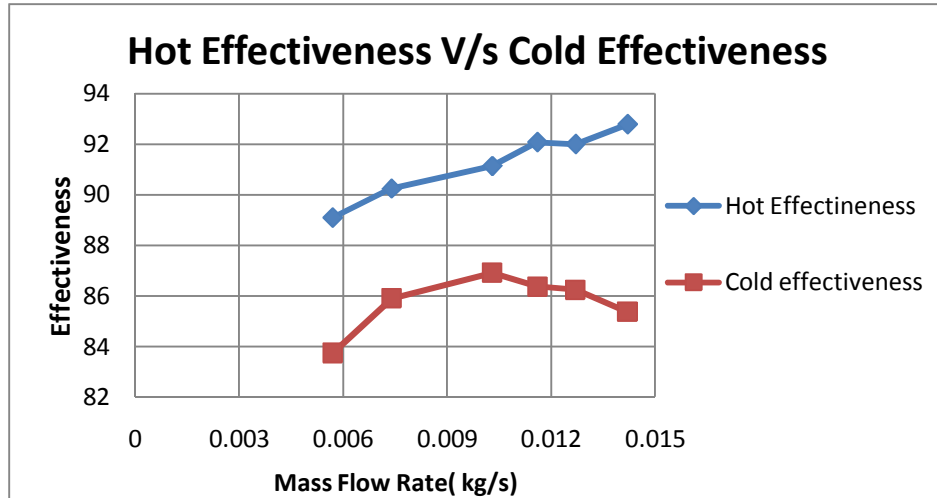


Fig. 5.5 Variation of Hot and Cold effectiveness with mass flow rate (hot inlet temperature of 96°C)

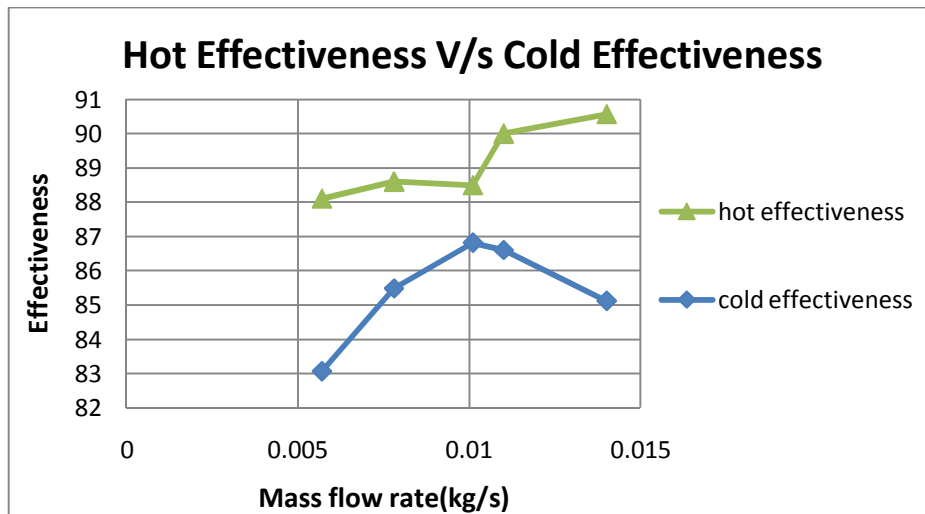


Fig. 5.6 Variation of Hot and Cold effectiveness with mass flow rat (hot inlet temperature of 66°C)

Figure 5.5 and 5.6 show how the experimental hot and cold effectiveness varies with the mass flow rate for hot inlet temperature of 96 and 66°C respectively. It is seen that both hot and

cold effectiveness increases with increasing mass flow rate and try to approach other and there is an optimum mass flow rate for each hot inlet temperature at which the gap between the two effectiveness is minimum and then again increases. Also after the optimum point the cold effectiveness again decreases, this is because a heat exchanger is designed for a particular mass flow rate and inlet temperatures at which it gives maximum effectiveness, after which its performance deteriorates. Also the imbalance increases because of heat loss to the environment as we are not able to provide the complete insulation. It can also be seen from the graphs that at lower hot inlet temperature the imbalance i.e. difference between the two effectiveness is less as compared to the imbalance at high temperatures.

5.5 Variation of Pressure Drop with Mass Flow Rate

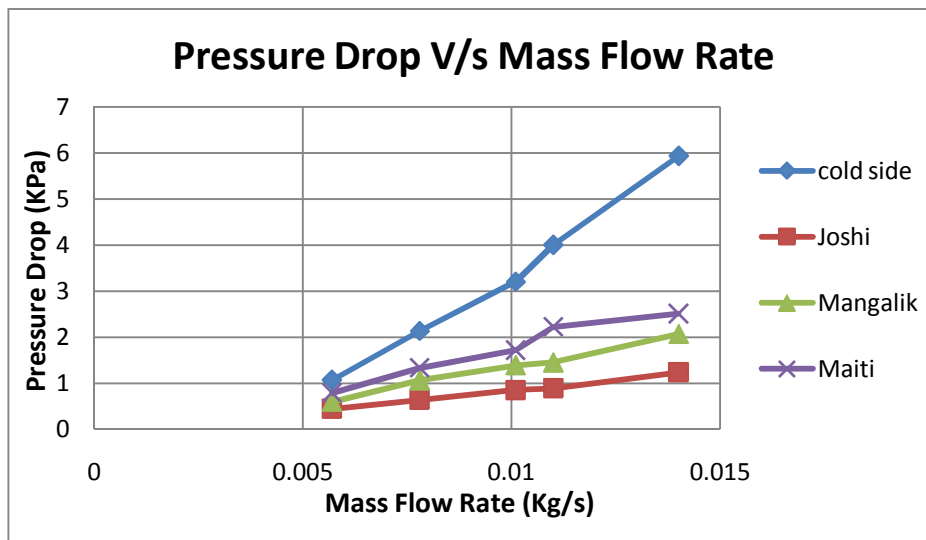


Fig. 5.7 Variation of pressure drop with mass flow rate

Figure 5.7 shows how the pressure drop in the heat exchanger varies with varying mass flow rate and also the comparison between experimental and theoretical pressure drop. It can be seen that the pressure drop increases with mass flow rate for each case. However the experimental pressure drop is much more as compared to the theoretical pressure drop because in theoretical calculations we have not taken in to account the pressure drop taking place in piping's and also the manufacturing irregularities and header losses.

CHAPTER 6

Conclusions

CONCLUSIONS

The hot test is conducted to determine the thermal performance parameters of the available plate fin heat exchanger at different mass flow rates and two different hot inlet temperatures of 96 and 66°C. An average effectiveness of 91% is obtained. It is found in both the cases that the effectiveness and overall thermal conductance increases with increasing mass flow rate. It is also found that hot fluid effectiveness increases with flow rate of the fluid and agrees within 4% with the effectiveness value calculated by different correlations and that obtained by using the simulation software, Aspen. Also the pressure drop increases with increasing mass flow rate and experimental values are more as compared to theoretical results because the losses in pipes and manufacturing irregularities have not been taken into account.

For a particular hot inlet temperature there is an optimum mass flow rate at which the difference between the hot and cold effectiveness of the heat exchanger is minimum and at this point the imbalance is also minimum. We found that the insulation which is provided in the heat exchanger has a significant effect on its performance. It is expected that the imbalance i.e. difference between the hot and cold end temperature can be brought to a minimum level if a perfect insulation like vacuum is provided.

6.1 Scope for Future Work

Present tests are conducted at room temperatures and in future we can perform the experiment at low temperatures in order to check the performance of the present heat exchanger for Cryogenic applications. In cold testing air at about 100K will be used as the cold fluid. In cold test in place of heater a cold box will be used.

References

REFERENCES

- [1] Patankar S. V. and Prakash C. 1981 An Analysis of Plate Thickness on Laminar Flow and Heat transfer in Interrupted Plate passages. *International Journal of Heat and Mass Transfer* 24: 1801-1810.
- [2] Joshi H. M. and Webb R. L. 1987. Heat Transfer and Friction in Offset Strip Fin Heat Exchanger, *International Journal of Heat and Mass Transfer*. 30(1): 69-80
- [3] Suzuki, K., Hiral, E., Miyake, T., Numerical and Experimental studies on a two Dimensional Model of an Offset-Strip-Fin type Compact Heat Exchanger used at low Reynolds Number. *International Journal of Heat and Mass Transfer* 1985 28(4) 823-836.
- [4] Tinaut F. V., Melgar A. and Rehman Ali A. A. 1992 Correlations for Heat Transfer and Flow Friction Characteristics of Compact Plate Type Heat Exchangers. *International Journal of Heat and Mass Transfer*. 35(7):1659:1665
- [5] Manglik and Bergles A. E. 1995 Heat Transfer and Pressure drop Correlations for Rectangular Offset Strip Fin Compact Heat Exchangers. *Experimental Fluid Science* 10:171-180.
- [6] Hu S and Herold K. E. 1995a Prandtl Number Effect on Offset Strip Fin Heat Exchanger Performance: Predictive Model for Heat Transfer and Pressure Drop. *International Journal of Heat and Mass Transfer* 38(6) 1043-1051
- Hu S and Herold K. E. 1995b Prandtl number Effect on Offset Strip Fin Heat Exchanger Performance: Experimental Results. *International Journal of Heat and Mass Transfer* 38(6) 1053-1061.
- [7] Zhang L. W., Balachandar S., Tafti D. K. and Najjar F. M. 1997. Heat Transfer Enhancement Mechanisms in Inline and Staggered Parallel Plate Fin Heat Exchanger. *International Journal of Heat and Mass Transfer* 40(10):2307-2325

- [8] Dejong N. C., Zhang L. W., Jacobi A. M., Balchandar S. and Tafti D. K. 1998. A Complementary Experimental and Numerical Study of Flow and Heat Transfer in Offset Strip Fin Heat Exchangers. *Journal of Heat Transfer* 12:690:702
- [9] Bhowmik H., Kwan- Soo Lee 2009. Analysis of Heat Transfer and Pressure Drop Characteristics in an Offset Strip Fin Heat Exchanger. *International Journal of Heat and Mass Transfer* 259-263
- [10] Saidi A. and Sudden B. 2001. A Numerical Investigation of Heat Transfer Enhancement in Offset Strip Fin Heat Exchangers in Self Sustained Oscillatory Flow. *International Journal of Numerical Methods for Heat and Fluid Flow*. 11(7): 699-716
- [11] Dong J., Chen J., Chen Z. and Zhou Y. 2007. Air Side Thermal hydraulic Performance of Offset Strip Fin Heat Exchangers Fin Alumunium Heat Exchangers. *Applied Thermal Engineering* 27:306-313
- [12] Michna J. G., Jacobi A. M. and Burton L. R. 2005. Air Side Thermal- Hydraulic Performance of an Offset Strip Fin Array at Reynolds Number up to 12, 0000. *Fifth International Conference on Enhanced Compact and Ultra Compact Heat Exchangers. Science, Engineering and Technology* 8-14.
- [13] Prabhat Gupta, Atrey M. D. Performance Evaluation Of Counter Flow Heat Exchangers Considering the Heat In Leak and Longitudinal Conduction for Low Temperature applications. *Cryogenics* Volume 40, issue 7, Pages 469-474.
- [14] Barron R. F., *Cryogenic Heat Transfer*, Taylor and Francis (1999) 311-318.
- [15] Shah R. K. and Sekulic D. P. *Fundamentals of Heat Exchangers*, John Willey & Sons Inc., pp 10-13
- [16] Kays W. M. and London A. L. *Compact Heat Exchangers*. 2nd Edition, McGraw-Hill, New York, 1964
- [17] Weiting A. R.1975. Empirical Correlations for Heat Transfer and Flow Friction Characteristics of Rectangular Offset strip Fin Plate Fin Heat Exchangers. *Transactions of ASME, Journal of Heat Transfer* 97:488-497

[18] Manson S. V. Correlations of Heat Transfer Data and of Friction Data for Interrupted Plane Fins Staggered in successive Rows NACA Technical Note 2237(1950)

[19] Maiti D.K. Heat Transfer and Flow Friction Characteristics of Plate Fin Heat Exchanger Surfaces- A Numerical Study PhD Dissertation Indian Institute of Technology, Kharagpur (2002)

[20] DURMAZ, Gurcan, Experimental and Numerical Analysis of Heat Transfer Performance of Offset Strip Fins, Master of Science thesis, The Graduate School Of Engineering and Science of IZMIR Institute of Technology;2009